Dalton Transactions



PAPER

View Article Online
View Journal | View Issue



Cite this: *Dalton Trans.*, 2025, **54**, 9949

Manganese germylene complexes: reactivity with dihydrogen, isonitriles, and dinitrogen†

Jeffrey S. Price and David J. H. Emslie *

The manganese germylene-hydride complexes $[(dmpe)_2MnH(=GeR_2)]$ (1a: R = Ph, 1b: R = Et) reacted with H_2 (approx. 1.5 atm) to afford the 'germyl dihdyride' species [(dmpe)₂MnH₂(GeHR₂)] (2a: R = Ph, 2b: R = Et) as an equilibrium mixture with the starting material (1a-b). In solution, 2a-b exist as a mixture of isomers where the major isomer (71–84%) is a trans hydrogermane hydride complex trans-[(dmpe)₂MnH (HGeHR₂)] (transHGe-2a-b). The minor isomer of 2a-b is tentatively assigned as the cis germyl dihydrogen complex cis-[(dmpe)₂Mn(GeHR₂)(H₂)] (cis-2a-b), possibly in rapid equilibrium with a small amount of the germanate complex [(dmpe)₂Mn(H₂GeHR₂)] (central-2a-b). DFT calculations were employed to gain insight into the nature of bonding in the isomers of 2a-b, and an X-ray crystal structure was obtained for trans-[(dmpe)₂MnH(HGeHEt₂)] (transHGe-2b) which co-crystallized with 1b. Reactions of 1a-b with D₂ suggest a pathway that proceeds via conversion of 1a-b to a 5-coordinate germyl intermediate $[(dmpe)_2Mn(GeHR_2)]$ (A) prior to reaction with H_2/D_2 . Providing support for this pathway, intermediate A (R = Ph) was trapped via reactions of 1a with isonitriles, affording the manganese(i) germyl isonitrile complexes [(dmpe)₂Mn(GeHPh₂)(CNR)] (**3a**: R = t Bu, **3b**: R = o -xylyl, and **3c**: R = n Bu). These complexes formed as a mixture of cis and trans isomers, and X-ray quality crystals were obtained for cis-3a, cis-3b and trans-3c. Complexes 1a-b also reacted slowly with dinitrogen at room temperature to afford germyl dinitrogen complexes $[(dmpe)_2Mn(GeHR_2)(N_2)]$ (5a: R = Ph, 5b: R = Et). Compounds 5a-b were initially formed as cis isomers, but the trans isomer is the thermodynamic product in each case, and the cis and trans isomers were crystallographically characterized for both 5a and 5b. X-ray crystallography, IR spectroscopy, and DFT calculations were employed to compare metal-dinitrogen bonding in the cis and trans isomers of 5a-b. The silyl dinitrogen derivative [$(dmpe)_2Mn(SiHPh_2)(N_2)$] (6) was also generated as a mixture of the cis and trans isomers, and the trans isomer was structurally characterized. The trans isomers of **5b** and **6** show $^{55}Mn-^{31}P$ coupling in the $^{31}P\{^{1}H\}$ and $^{55}Mn\{^{1}H\}$ NMR spectra, affording 1:1:1:1:1:1:1 sextets and 1:4:6:4:1 quintets, respectively.

Received 1st May 2025, Accepted 2nd June 2025 DOI: 10.1039/d5dt01025j

rsc.li/dalton

Introduction

Germylene (:GeR₂) ligands in transition metal complexes can serve as highly reactive sites, including for small molecule activation. Lexamples of reactivity involving germylene ligands include coordination of nucleophiles to germanium, Lewis base (RCN or pyridine) addition to a germylene hydride complex to afford a germyl complex, and migration of a hydrogen substituent in a GeHR ligand to the metal center to form a metallogermylene (L_x HM-Ge-R). Germylene to germylyne transformations have also been demonstrated by

Department of Chemistry, McMaster University, 1280 Main St West, Hamilton, Ontario, L8S 4M1, Canada. E-mail: emslied@mcmaster.ca

†Electronic supplementary information (ESI) available: Overview of literature Mn(i) dinitrogen chemistry, selected NMR and IR spectra, SCD and PXRD data, and DFT results. CCDC 2447494–2447503. For ESI and crystallographic data in CIF or other electronic format see DOI: https://doi.org/10.1039/d5dt01025j

α-chloride migration, 12 loss of a hydride ligand and an alkyl substituent on germanium (as HR, where R = CH₂PMe₂),¹³ or dehydrogenation of an [LxMH(=GeHR)] complex by reaction with an NHC, isocyanate or nitrile. 7,8,14 Additionally, various reactions of $[L_xMH(=GeHR)]^{x+}$ complexes with unsaturated substrates have been reported. For example, cationic complexes reacted with alkenes and alkynes to form hydrogermylation products, 15 and neutral complexes reacted with aldehydes and ketones $(R_2^{\prime}C=0)$ to afford $[L_rMH(=Ge(OCHR_2^{\prime})R)]$ (the latter reactions were proposed to proceed by R'2C=O coordination to Ge, nucleophilic attack at the carbonyl carbon by the metal hydride to form a germyl intermediate, and subsequent 1,1-deinsertion).^{5,9} Furthermore, $[L_xMH(=GeHR)]$ complexes reacted with isocyanates or isothiocyanates to afford metallacyclic products containing a 5-membered MGeECN (E = O or S) or MGeNCS ring. 8,9,16 Addition of H2O, MeOH, or NH3 across a germylene M=Ge bond has also been reported, affording germyl hydride complexes with an OH, OMe or NH2 substituPaper **Dalton Transactions**

ent on germanium, 17,18 and 2 + 2 cycloaddition has been observed or proposed in reactions of germylene complexes with CO₂ and isothiocyanates. 9,19 Such reactivity offers many avenues for Ge incorporation into larger molecules. However, compared to lighter silylene^{2,20-23} and (especially) carbene²⁴⁻²⁶ complexes, the reactivity of transition metal germylene species is far less explored.

Recently, our group isolated the first terminal base-free germylene complexes of manganese, [(dmpe)₂MnH(=GeR₂)] (1a: R = Ph, 1b: R = Et), by hydrogermane addition to Girolami and Wilkinson's^{27,28} manganese hydride complex [(dmpe)₂MnH (C₂H₄)] (top of Scheme 1),²⁹ which serves as a source of [(dmpe)₂MnEt].³⁰ While **1a-b** did not react with additional equivalents of H2GeR2, the monosubstituted derivative $[(dmpe)_2MnH(=GeH^nBu)]$ (1c) reacted with excess H_3Ge^nBu to produce a solution containing 1c and H₃GeⁿBu in equilibrium with the products of hydrogermane addition; trans- $[(dmpe)_2Mn(GeH_2^nBu)(HGeH_2^nBu)]$ and $mer-[(dmpe)_2MnH$ (GeH₂ⁿBu)₂] (bottom of Scheme 1).²⁹ This reactivity suggests that the germylene-hydride complex 1c exists in equilibrium with an undetected 5-coordinate manganese(1) germyl complex [(dmpe)₂Mn(GeH₂ⁿBu)] which is responsible for the observed reactivity with hydrogermanes.

We have previously reported the manganese silylene complexes [(dmpe)₂MnH(=SiR₂)],³¹ which are lighter congeners of 1a-b, and their diverse (and in some cases highly unusual) reactivity with small molecules including H2, H2SiR2, C2H4, CO₂, and C(NⁱPr)₂. 31-34 Herein, we report reactions of the germylene-hydride complexes [(dmpe)₂MnH(=GeR₂)] (1a-b) with dihydrogen, isonitriles, and dinitrogen. Literature examples of reactivity of metal germylene complexes with these small molecules are scarce, though reactions with dihydrogen to form germyl hydride complexes have been reported for [(Et₃P)₂Pt $(=Ge\{N(SiMe_3)_2\}_2)]$, ¹⁹ the heterobimetallic complex $[(OC)Rh(\mu H)(\mu\text{-dppm})_2(\mu\text{-GePh}_2)Ir(CO)[CF_3SO_3],^{35}$ $[(Cy_3P)_2RuH_2(H_2)$ (=GePh₂)] (in this case affording a mixture of germyl hydride and hydrogermane complexes), 36 [(Dipp2ArMe2P)Pt{=GeCl

$$R = Ph (1a) \text{ or Et } (1b)$$

$$R = Ph (1a) \text{ or Et } (1b)$$

$$R = Ph (1a) \text{ or Et } (1b)$$

$$R = Ph (1a) \text{ or Et } (1b)$$

$$R = Ph (1a) \text{ or Et } (1b)$$

$$R = Ph (1a) \text{ or Et } (1b)$$

$$R = Ph (1a) \text{ or Et } (1b)$$

Scheme 1 Top: Synthesis of manganese germylene-hydride complexes $[(dmpe)_2MnH(=GeR_2)]$ (1a: R = Ph, 2b: Et). Bottom: Equilibria observed between germylene-hydride complex [(dmpe) $_2$ MnH(=GeH n Bu)] (1c) and the Mn(i) germyl complexes trans-[(dmpe)₂Mn(GeH₂ⁿBu)(HGeH₂ⁿBu)] mer-[(dmpe)₂MnH(GeH₂ⁿBu)₂] upon exposure excess to hydrogermane.²⁹

 $(^{Dipp2}Ar)\}],^{18}$ and $[(IPr)Ni(\kappa^2-P,Ge-Ph_2PCH_2Si^iPr_2N(Dipp))]$ GeAr)].³⁷ A reaction of the titanium germylene complex [(THF) $TiCp_2{=GeSi(SiMe^tBu_2)Si(SiMe^tBu_2)_2Si(SiMe^tBu_2)}$ with an isonitrile has also been reported, but simply resulted in substitution of the THF co-ligand.38

Results and discussion

Reactions with H₂

Solutions of the manganese germylene-hydride complexes trans- $[(dmpe)_2MnH(=GeR_2)]$ (1a: R = Ph, 1b: R = Et)²⁹ reacted with H_2 (~1.5 atm) at room temperature to afford the 'germyl dihydride' complexes $[(dmpe)_2MnH_2(GeHR_2)]$ (2a: R = Ph, 2b: R = Et); Scheme 2. These reactions only progressed to 87% (2a) or 73% (2b) conversion, reaching equilibrium with 1a-b and H₂ within 3 days. This reactivity contrasts that of the silicon analogues which proceeded to completion (within a few minutes (R = Ph) or 24 hours (R = Et)) to form 'silyl dihydride' complexes that are stable towards H₂ elimination. 31,33

At room temperature, compounds 2a-b gave rise to a single hydride signal in the ¹H NMR spectrum and one broad ³¹P{¹H} NMR signal. However, upon cooling to 176 K, three ¹H NMR signals (2a: 5:5:2, 2b: 4:4:3 relative integration) were observed in the low-frequency (<0 ppm) region, and the 31P {1H} NMR spectrum contained one intense and three low intensity peaks (see Fig. 1 for 2a), indicative of a major and a minor isomer (vide infra).

$$R = Ph (1a) \text{ or Et (1b)}$$

$$R = Ph (1a) \text{ or Et (1b)}$$

$$R = Ph (transH_2-2a)$$

$$R = Ph (transHGe-2a)$$

$$R = Ph (transHGe-2a)$$

$$R = Ph (transHGe-2b)$$

$$R = Ph (cis-2a)$$

$$R = Ph (central-2a)$$

$$R = Ph (transHGe-2b)$$

germylene-hydride the $[(dmpe)_2MnH(=GeR_2)]$ (1a: R = Ph, 1b: R = Et) with dihydrogen to afford an equilibrium mixture containing isomers of [(dmpe)₂MnH₂(GeHR₂)] (2a: R = Ph, 2b: R = Et). The major isomer of 2a-b was identified as the trans-hydrogermane hydride complex transHGe-2a,b. For consistency with previous literature, the hydrogermane ligand in this isomer is drawn as a σ-complex, despite existing on a continuum between a sigma complex and a germyl dihydride species resulting from Ge-H bond oxidative addition.³⁹ The minor isomer of **2a-b** is tentatively assigned as the cis germyl dihydrogen complex cis-[(dmpe)2Mn(GeHR2)(H2)] (cis-2a-b), possibly in rapid equilibrium with a small amount of the germanate complex [(dmpe)₂Mn(H₂GeHR₂)] (central-2a-b; shown in gray); vide infra. The inset shows transH2 isomers which were not experimentally observed.

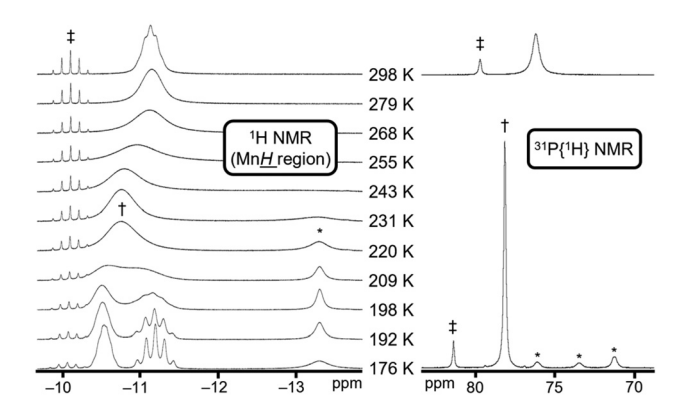


Fig. 1 Variable temperature ^1H NMR (500 MHz; left) and $^{31}\text{P}\{^1\text{H}\}$ NMR (202 MHz; right) spectra of the reaction mixture formed from the reaction of [(dmpe)₂MnH(=GePh₂)] (1a; ‡) with H₂ in d_8 -toluene (see Fig. S23† for $^{31}\text{P}\{^1\text{H}\}$ NMR spectra at all temperatures). This reaction affords the 'germyl dihydride' complex [(dmpe)₂MnH₂(GeHPh₂)] (2a), as a mixture of rapidly exchanging isomers, in slow equilibrium with 1a and H₂. Peaks attributed to *transHGe-2a* are indicated with the symbol †, whereas those for an isomer with a disphenoidal arrangement of the dmpe ligands (tentatively identified as *cis-2a*, possibly in rapid equilibrium with a small amount of *central-2a-b*; *vide infra*) are indicated with the symbol *.

The dominant isomer of 2a-b in solution (84% for 2a, 71% for 2b) is the trans-hydrogermane hydride complex trans- $[(dmpe)_2MnH(HGeHR_2)]$ (transHGe-2a: R = Ph, transHGe-2b: R = Et). At 176 K, this isomer gave rise to a single sharp peak in the ${}^{31}P{}^{1}H}$ NMR spectrum (at 78 ppm (2a) or 76 ppm (2b)), indicative of an equatorial arrangement of the two dmpe ligands, and requiring rapid rotation of the hydrogermane ligand (which could alternatively be viewed as a hydride and a germyl ligand that are closely interacting) on the NMR timescale. ¹H NMR signals for the major isomer include a single terminal GeH peak at 6.1 (2a) or 4.6 (2b) ppm, accompanied by two low frequency signals (-10.5 and -11.2 ppm for 2a, -11.0 and -11.3 ppm for 2b). In each case, the lower frequency signal is a well-defined quintet (${}^2J_{\rm H,P}$ = 56–58 Hz) arising from the hydride ligand trans to the hydrogermane (positioned cis to four equivalent phosphines), whereas the higher frequency signal corresponds to the H atom of the manganese-coordinated Ge-H bond.

At 176 K, the lower symmetry isomer of 2a-b gave rise to single Mn*H* (–13.3 (2a) or –13.9 (2b) ppm) and terminal Ge*H* (6.05 (2a) or 4.55 (2b) ppm) ¹H NMR environments integrating to 2H and 1H, respectively, and three ³¹P{¹H} NMR signals with 1:1:2 integration, indicative of a disphenoidal arrangement of the phosphine donors (71–76 (2a) or 72–75 (2b) ppm). These data are consistent with two potential isomers: (a) *cis*-[(dmpe)₂Mn(GeHR₂)(H₂)] (*cis*-2a-b) containing *cis*-disposed dihydrogen and germyl ligands, or (b) [(dmpe)₂Mn(H₂GeHR₂)] (*central*-2a-b) featuring an anionic germanate (H₂GeHR₂) ligand that coordinates to manganese *via* the two newlyformed Ge–H bonds (the germanate ligand could alternatively be viewed as a germyl ligand interacting closely with two flanking hydride ligands). X-ray crystal structures have been

reported for Ru⁴⁰ and Nb⁴¹ complexes existing as germyl dihydrogen or germyl dihydride complexes, similar to the *cis* and *central* isomers of **2a-b**, respectively.

Maintaining a solution containing **1b** and **2b** in hexanes under an atmosphere of dihydrogen at −78 °C afforded crystals of *trans*-[(dmpe)₂MnH(HGeHEt₂)] (*transHGe*-2b) co-crystallized with the germylene-hydride starting material [(dmpe)₂MnH (≡GeEt₂)] (**1b**) in a 0.46 : 0.54 ratio (Fig. 2). To the best of our knowledge, this is the first X-ray crystal structure of a hydrogermane manganese complex, and a rare example of a monometallic transition metal complex featuring a terminal hydrogermane ligand. ^{39,42-45} However, due to co-crystallization of **1b** with *transHGe*-2b as well as disorder in the hydrogermane ligand in *transHGe*-2b (which together results in three overlapping Ge ellipsoids), the structure is only suitable to establish connectivity.

DFT calculations (ADF/AMS, gas phase, all-electron, TZ2P, PBE, ZORA, D3-BJ) were carried out on the aforementioned *transHGe*, *cis*, and *central* isomers of germyl dihydride complexes **2a-b**, as well as an isomer with *trans*-disposed H₂ and germyl ligands, *trans*-[(dmpe)₂Mn(GeHR₂)(H₂)] (*transH*₂-**2a-b**); Fig. 3and S175, Table S13.† These calculations identified *transHGe*-**2a-b** (the major species observed in solution by NMR spectroscopy) as the global minimum, and ΔG_{176K} (176 K is the lowest temperature at which decoalesced NMR spectra were obtained) for conversion of *transHGe*-**2a-b** to the other isomers was 9–11 kJ mol⁻¹ for *cis*-**2a-b** and *central*-**2a-b**, and 14–16 kJ mol⁻¹ for *transH*₂-**2a-b** (Fig. 4).

The calculated structures of *transHGe-2a-b* feature a hydrogermane ligand which has undergone substantial but incomplete Ge–H bond oxidative addition. The terminal Mn–H, bridging Mn–H (bridging between Mn and Ge), and terminal Ge–H distances are 1.54–1.55, 1.56–1.57, and 1.58 Å, with Mayer

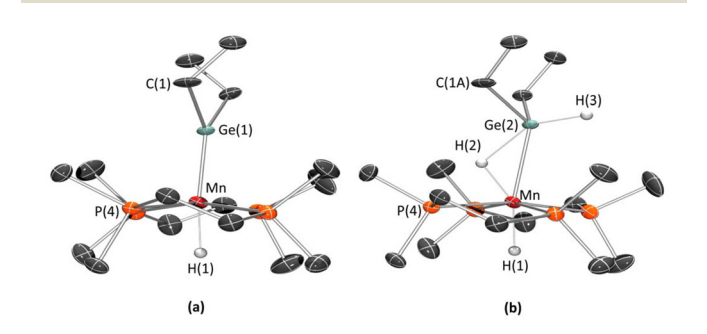


Fig. 2 Views of the (a) [(dmpe)₂MnH(≔GeEt₂)] (1b) and (b) transHGe-[(dmpe)₂MnH(HGeHEt₂)] (transHGe-2b) components in crystals containing both of these species. The germanium-containing ligand in the structure is disordered over three parts − the germylene (GeEt₂) ligand in 1b (54.2(3)% occupancy; view a), the hydrogermane (HGeHEt₂) ligand in transHGe-2b (40.2(3)% occupancy; view b), and another orientation of the hydrogermane ligand in transHGe-2b with 5.6(3)% occupancy (not shown; H atoms on this minor disorder component were not located from the difference map). Most hydrogen atoms have been omitted for clarity, with the exception of those on Mn and Ge which were located from the difference map and refined isotropically. Ellipsoids are shown at 50% probability.

transHGe-2b central-2b

Fig. 3 Geometry optimized DFT calculated structures for the transHGe, central, cis, and $transH_2$ isomers of [(dmpe)₂MnH₂(GeHEt₂)] (2b), with P-methyl groups and most hydrogen atoms omitted for clarity. Spheres represent Mn (red), Ge (green), P (orange), and H (white), whereas carbon atoms are represented by grey vertices. Solid bonds are those with Mayer bond orders >0.40, while dashed bonds are those with Mayer bond orders between 0.13 and 0.23.

transH₂-2b

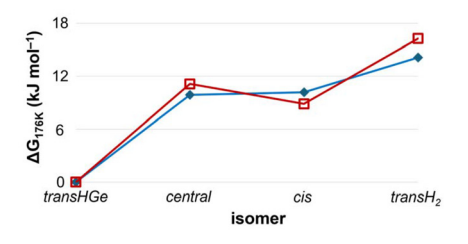


Fig. 4 DFT calculated Gibbs free energy changes (at 176 K) for isomerization of trans-[(dmpe)₂MnH(HGeHR₂)] (transHGe-2a: R = Ph, transHGe-2b: R = Et) to the central, cis and transH₂ isomers. Values for 2a are shown as red hollow squares, and values for 2b are shown as blue diamonds.

bond orders of 0.82–0.83, 0.65, and 0.84 respectively, and the bridging Ge–H distances are 2.00–2.08 Å with Mayer bond orders of 0.22–0.23 (Fig. 5; left). These bridging Ge–H distances are similar to those in Mo (2.08(6) Å), ³⁹ Rh (2.13(3) Å), ⁴² and Pd (2.04(8) Å) ⁴³ complexes that are described as σ -hydrogermane complexes with partial Ge–H bond oxidative addition. By contrast, they are elongated relative to those in a cationic Pt(II) σ -hydrogermane complex (XRD: 1.78(4) Å, DFT: 1.79 Å) which would be expected to feature very limited Ge–H bond oxidative addition. ⁴⁴ Conversely, they are shorter than the Ge–H distances (2.17(4)–2.23(6) Å) in a series of nickel complexes described as containing germyl and hydride ligands with a significant interligand interaction. ³⁷

The Mn-Ge distances in *transHGe-2a-b* are 2.43 and 2.46 Å, with Mayer bond orders of 0.74 and 0.78 (Fig. 5). These

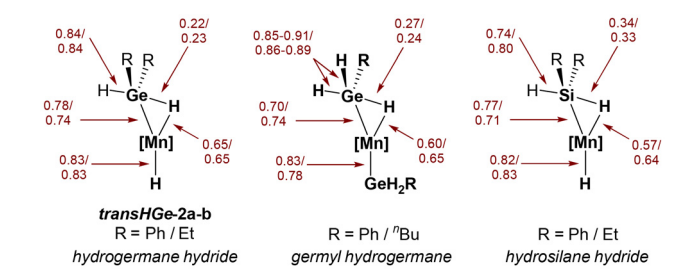


Fig. 5 Mayer bond orders for Mn–E, Mn–H and E–H bonds (E = Ge or Si) in trans-[(dmpe)₂MnH(HGeHR₂)] (transHGe-2a–b) compared with those previously reported for the germyl hydrogermane complexes trans-[(dmpe)₂Mn(GeH₂R)(HGeH₂R)] (R = Ph or n Bu)²⁹ and the hydrosilane hydride complexes trans-[(dmpe)₂MnH(HSiHR₂)] (R = Ph or Et).³³ In all cases [Mn] is Mn(dmpe)₂, and the same computational method (ADF/AMS, gas phase, all-electron, TZ2P, PBE, ZORA, D3-BJ) was employed.

bond distances are significantly longer than that in germylene complex ${\bf 1a}$ (2.2636(4) Å), 29 but are comparable with those calculated for the three higher energy isomers (the *cis*, *central* and *trans*-H₂ isomers) of ${\bf 2a-b}$; 2.39–2.49 Å, with Mayer bond orders of 0.69–0.85 (Table S13†). They are also similar to the crystallographically determined Mn–Ge distances in the germyl complexes [(dmpe)₂Mn(GeHR₂)(L)] (R = Ph or Et, L = CNR or N₂) discussed below (2.475(1)–2.538(9) Å). Similarities between the transition metal–germanium distances in germyl and hydrogermane complexes have previously been reported. For example, DFT calculations on [(κ^2 -H₂PCH₂CH₂PH₂)₂Mo (CO)(L)] (L = hydrogermane or germyl hydride) complexes afforded Mo–Ge distances that are marginally longer in the germyl hydride isomers (by 0.01–0.04 Å) than in the lowest energy hydrogermane isomers.³⁹

In Fig. 5, relevant Mayer bond orders in transHGe-2a-b are compared with those in the germyl hydrogermane complexes trans- $[(dmpe)_2Mn(GeH_2R)(HGeH_2R)]$ (R = Ph or ⁿBu), ²⁹ and the hydrosilane hydride complexes trans-[(dmpe)2MnH(HSiHR2)] (R = Ph or Et). 33 These comparisons reveal (a) very similar Mn-H, Mn-Ge and Ge-H bond orders in transHGe-2a-b and the germyl hydrogermane complexes, and (b) lower $E-H_{Mn}$ (E = Ge or Si) bond orders in transHGe-2a-b compared to the hydrosilane hydride analogues (especially considering that the Mayer bond orders are marginally higher for the Ge-H versus Si-H bonds in free H₂GeEt₂ and H₂SiEt₂, respectively; 0.92 vs. 0.91), indicative of a greater degree of E-H bond oxidative addition in transHGe-2ab. The trend in the relative degree of Si-H vs. Ge-H oxidative addition mirrors that previously noted for [(bisphosphine)2Mo (CO)(HER₃)] (E = Si, Ge) complexes.³⁹ The structures of the silicon analogues of transHGe-2a-b provide an important reference point given that the negative $J_{^{29}Si,^{1}H}$ coupling constants for these complexes (-41 and -54 Hz; determined using ²⁹Si_edited ¹H-¹H COSY NMR spectroscopy) are indicative of dominant ¹J coupling (rather than ²*J* coupling which would give rise to a positive coupling constant), supporting the non-classical nature of the complexes; $J_{^{29}Si,^{1}H}$ values ranging from 0 to -70 Hz are commonly considered to indicate activated Si-H bonds in nonclassical hydrosilane complexes. 46-48

Dalton Transactions Paper

Reactions with D₂

On a timescale of hours, reactions of [(dmpe)₂MnH(=GeR₂)] (1a-b) with D_2 in C_6D_6 or d_8 -toluene cleanly produced $[(dmpe)_2MnD_2(GeHR_2)]$ (d₂-2a: R = Ph, d₂-2b: R = Et), with hydrogen located exclusively in the terminal GeH bond in both (or all) isomers of the complexes. This reactivity with D₂ is analogous to that of the silvlene complex [(dmpe)₂MnH (=SiEt₂)],³¹ and suggests that the formation of 2a-b proceeds via initial isomerization of 1a-b to a 5-coordinate germyl intermediate [(dmpe)₂Mn(GeHR₂)] (A), followed by H₂/D₂ oxidative addition. This contrasts the reactivity of D2 with the heterobimetallic μ-germylene hydride complex [(OC)Rh(μ-H)(μdppm)₂(µ-GePh₂)Ir(CO)]⁺, which occurred rapidly at room temperature to generate [(OC)Rh(μ-H)(μ-dppm)₂(μ-GeDPh₂)IrD (CO)]⁺ as the primary product (although an equal distribution of H/D across all three sites was reported after 2 days at room temperature).35

After 3 days in d_8 -toluene, the reaction of 1a with D_2 (4-6 equiv.) to form d_2 -2a is at or near equilibrium, and low temperature ³¹P{¹H} NMR spectroscopy revealed that the fast equilibrium between the major transHGe isomer‡ and the minor species (the cis or central isomer, or a rapidly exchanging mixture of both) is shifted further towards the minor species compared with the reaction with H2 to form 2a, affording an equilibrium isotope effect (EIE = K_H/K_D) of 0.63-0.69 over the temperature range 176-198 K. Room temperature H/D scrambling (between the Ge-H and Mn-D positions in $[(dmpe)_2MnD_2(GeHR_2)]$) was not observed for d_2 -2a, but heating overnight at 55-60 °C afforded baseline MnH134 signals (<2% relative to the GeH signals).

By contrast, allowing the reaction of 1b with D₂ (4 equiv.) to proceed for 4 days in d_8 -toluene at room temperature afforded d_2 -2b as well as other isotopologues (d_3 -2b, and smaller amounts of d_1 -2b and 2b), giving rise to both GeH and MnH signals in the ¹H NMR spectrum, as well as some HD and H₂. These observations are consistent with slow hydrogermane (e.g. HDGeEt₂) dissociation and re-coordination from d_n -2b (perhaps from the *transHGe* isomer) as well as pathways involving D₂/HD/H₂ dissociation and re-coordination.

A low temperature (176 K) ¹H{³¹P} NMR spectrum of the mixture of 2b, d_1 -2b, d_2 -2b, and d_3 -2b features a 1:1:1 triplet at -13.94 ppm overlapping with a broad singlet at slightly higher frequency (Fig. 6). These signals correspond to the minor isomer of d_{n} -2b (n = 0-2), and the coupling constant for the 1:1:1 triplet is 28 Hz, indicative of an HD ligand. 49,50 This signal is proposed to arise from the cis isomer of $[(dmpe)_2Mn(GeXEt_2)(HD)]$ {X = D (d_2 -2b) and H (d_1 -2b); see Fig. 6}, and the 28 Hz coupling constant almost exactly

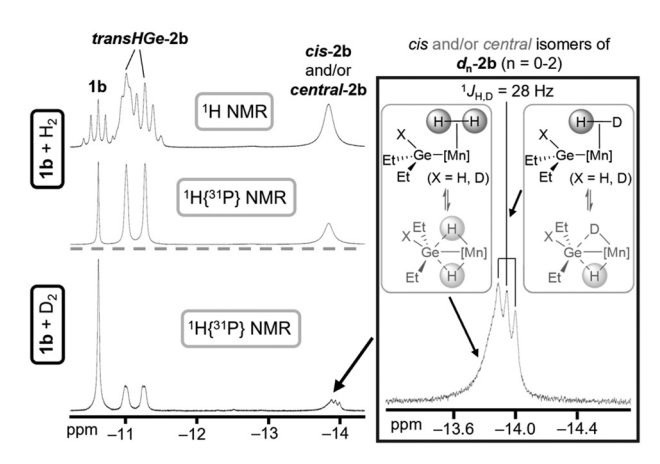


Fig. 6 ¹H and ¹H{³¹P} NMR spectra (176 K; 500 MHz) of the mixtures formed from the room temperature reactions of [(dmpe)₂MnH(=GeEt₂)] (1b) with (top) H_2 or (bottom) D_2 in d_8 -toluene after 4 days. The reaction with D_2 afforded a mixture of d_2 -2b and d_3 -2b, as well as smaller amounts of d_1 -2b and 2b. Only the low frequency region of the spectra is shown (which does not contain any signals for d_3 -2b or isomers/isotopomers of d_2 -2b with a terminal Ge-H bond). The expansion on the right shows the low-frequency ¹H{³¹P} signal for the minor isomer(s) of d_n -2b (n = 0-2), which consists of a 1:1:1 triplet overlapping with a broad singlet. The 1:1:1 triplet is proposed to arise from isomers containing an HD ligand (d_2 -2b where X = D and d_1 -2b where X = H; X is the terminal H/D substituent on germanium), while the broad singlet is proposed to arise from isomers containing an H_2 ligand (d_1 -2b where X = D and 2b). The H₂ and HD complexes (cis isomers) may or may not be in rapid equilibrium with a small amount of a germanate species (central isomers). $[Mn] = (dmpe)_2 Mn$.

matches that predicted49,51 based on the calculated H-H distance of 0.95 Å in cis-2b. The aforementioned broad singlet is proposed to arise from the cis isomer of [(dmpe)₂Mn(GeXEt₂) (H_2)] {X = D $(d_1$ -2b) and H (2b)}, both of which contain an H_2 ligand (see Fig. 6).

While these data suggest that the minor isomer of 2b is the cis-dihydrogen complex (the cis isomer) rather than a germanate complex (the *central* isomer), the presence of a small amount of the central isomer (in rapid equilibrium with the cis isomer) cannot be excluded, given (a) the very similar energies of the cis and central isomers of 2a-b in DFT calculations, and (b) potential differences in the position of any cis-central equilibrium in reactions involving HD versus H2 or D2 (especially considering that low-temperature reactions with H₂/D₂ to form an H₂/D₂ complex typically exhibit a substantial inverse equilibrium isotope effect). 52,53 This situation contrasts that for silicon analogues of 2a-b, where the spectroscopically identified isomers were trans-[(dmpe)2MnH(HSiHRR')] (a transHSi isomer) and the silicate complex [(dmpe)2Mn(H2SiHRR')] (a central isomer), both of which were crystallographically characterized.31

Reactions with isonitriles

The putative 5-coordinate germyl intermediate [(dmpe)₂Mn (GeHR₂)] (A) was trapped using isonitriles. For example, exposure of $[(dmpe)_2MnH(=GePh_2)]$ (1a) to an excess of tert-

[‡]The ³¹P NMR signal for transHGe-[(dmpe)₂MnD(DGeHPh₂)] (d₂-transHGe-2a) is shifted 0.4 ppm to higher frequency than in the protio isotopomer transHGe-2a. This is relatively unusual, since secondary NMR isotopic shifts usually proceed to lower frequency upon substitution of a nearby atom with a heavier isotope. 134 The average ³¹P NMR environment observed at 298 K for all isomers of 2a, as well as 31P NMR signals for the minor species in solution, are too broad for a similarly small secondary NMR isotopic shift to be measured.

Scheme 3 Syntheses of manganese(i) germyl isonitrile complexes [(dmpe) $_2$ Mn(GeHPh $_2$)(CNR)] (3a–c; R = t Bu, Xyl or n Bu) and the previously reported 54 hydride complex [(dmpe) $_2$ MnH(CNXyl)] (4). Xyl = o-xylyl.

butyl isonitrile (CN⁶Bu) afforded the germyl isonitrile complex $[(dmpe)_2Mn(GeHPh_2)(CNR)]$ (3a: $R = {}^tBu)$ as a yellow solid in 42% yield (Scheme 3). Analogues of 3a featuring different isonitrile ligands (3b: R = o-xylyl, 3c: $R = {}^nBu)$ were also synthesized via the same route (Scheme 3) and characterized $in \ situ$ by NMR spectroscopy.§ The reactions to form 3a–c all proceeded to completion within 1 hour at room temperature.

In solution, two sets of NMR signals were observed for 3a-c (Table S12†), consistent with a high symmetry *trans* isomer containing an equatorial belt of dmpe ligands (one ³¹P{¹H} singlet was observed at 71–74 ppm), and a low symmetry *cis* isomer with multiple ³¹P NMR environments arising from disphenoidal dmpe coordination. The GeH signals in the ¹H NMR spectra range from 5.06–5.27 ppm for the *trans* isomers and 5.45–5.48 for the *cis* isomers. Initially formed solutions of 3a-c contain a mixture of *cis* and *trans* isomers in ratios ranging from 83:17 to 77:23, which remained unchanged overnight at room temperature (though a different ratio was observed in recrystallized samples of 3a and 3c due to preferential crystallization of the *cis* isomers).

§ The reaction mixture formed from n-butyl isonitrile and 1a contained a significant unidentified byproduct comprising ~30% of the mixture, which featured four 31P{1H} NMR environments and a very high frequency 1H NMR signal (consistent with a CH(=NR)¹³⁵ or GeHR²⁹ ligand). Removal of the solvent in vacuo followed by washing with hexanes and recrystallization from toluene layered with hexanes at −30 °C resulted in isolation (though not with analytical purity) of cis-3c. Selected NMR data for the unidentified impurity are as follows: 1H NMR (C₆D₆, 600 MHz, 298 K, integrals normalized to 1H for the peak at 11.60 ppm): δ 11.60 (d of d, 1H, $J_{H,P}$ 9.3 and $J_{H,P}$ 3.6 Hz), 7.89, 7.79 (2 × t, 2H, $J_{H,H}$ 7.1 Hz), 3.78, 3.59 (2 × m, 1H), 1.46 (d, 3H, $J_{H,P}$ 4.8 Hz), 1.33 (d, 3H, $J_{H,P}$ 5.1 Hz), 1.29 (d, 3H, $J_{H,P}$ 6.4 Hz), 1.10 (d, 3H, $J_{H,P}$ 5.9 Hz), 0.82 (d, 3H, $J_{H,P}$ 4.6 Hz). ¹³C{¹H} NMR (C₆D₆, 151 MHz, 298 K): δ 159.42, 158.79, 134.23, 133.69, 127.78, 127.69, 126.32, 125.95, 58.58 (9 × s), 35.79 (app. t, $J_{C,P}$ 22.1 Hz), 34.85 (d, $J_{C,P}$ 13.4 Hz), 33.88, 20.29 (2 \times m), 26.14 (d, $J_{\rm C,P}$ 9.1 Hz), 25.74 (d of d, $J_{\rm C,P}$ 12.8 and 6.9 Hz), 19.16 (d, $J_{\text{C,P}}$ 7.4 Hz). ³¹P{¹H} NMR (C₆D₆, 243 MHz, 298 K): δ 80.84, 72.74, 72.37, 62.64 (4 × s, 1P).

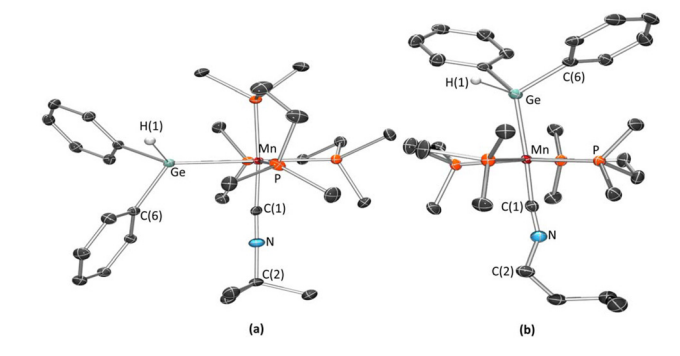


Fig. 7 X-ray crystal structures of (a) cis-[(dmpe)₂Mn(GeHPh₂)(CN^tBu)] (cis-3a) and (b) trans-[(dmpe)₂Mn(GeHPh₂)(CNⁿBu)] (trans-3c), with ellipsoids at 50% probability. Most hydrogen atoms have been omitted for clarity, except for those on Ge, which were located from the difference map and refined isotropically.

Heating the reaction mixture from the synthesis of $[(dmpe)_2Mn(GeHPh_2)(CNXyl)]$ (3b; Xyl = o-xylyl) resulted in slow formation of the previously reported⁵⁴ manganese(1) hydride complex $[(dmpe)_2MnH(o$ -xylyl)] (4) (70% conversion after heating for \sim 12 h at 100 °C) accompanied by unidentified byproducts; Scheme 3. Recrystallization from hexanes afforded X-ray quality crystals of 4, with an Mn–H distance of 1.75(7) Å, an Mn–C distance of 1.789(6) Å, a C–N distance of 1.221(8) Å, and a C–N–C angle of 160.4(5)° (Fig. S168†). An X-ray crystal structure of this complex was previously published⁵⁴ with a different unit cell (in a higher symmetry space group), featuring a perfectly straight Mn–C–N–C rod lying on a C_2 axis.

X-ray crystal structures were obtained for $3\mathbf{a}$ - \mathbf{c} ¶ as the *cis* $(3\mathbf{a}$ - $\mathbf{b})$ or *trans* $(3\mathbf{c})$ isomer; Fig. 7 and S167, Table S11.† In all cases, the hydrogen atoms on Ge were located from the difference map and refined isotropically. The Mn–Ge distances of 2.475(1)–2.481(1) Å (*cis* isomers of $3\mathbf{a}$ - \mathbf{b}) and 2.528(1) Å (*trans*- $3\mathbf{c}$) are at the higher end of the range previously reported for neutral manganese(i) germyl complexes (2.37–2.53 Å), ⁵⁵ and in each case, appreciable bending of the isonitrile ligands (C–N–C = 144.9(4)–172.6(3)°) was observed.

Reactions with N₂

While coordination of the highly donating isonitrile ligands to manganese(i) is not unexpected, similar reactivity was also observed with dinitrogen. The manganese germylene-hydride complexes trans-[(dmpe)₂MnH(=GeR₂)] (1a: R = Ph, 1b: R = Et)²⁹ reacted in solution with dinitrogen (~1.5 atm) at room temperature to afford solutions of the germyl-dinitrogen complexes [(dmpe)₂Mn(GeHR₂)(N₂)] (5a: R = Ph, 5b: R = Et); Scheme 4. These reactions are much slower than those involving isonitriles, reaching 95% (5a) or complete (5b) conversion

¶The X-ray crystal structure of 3b contains two independent and essentially isostructural molecules in the unit cell. One of these has disorder in the dmpe ligands which could not be completely modelled from the difference map. Therefore, only bond metrics for 3b from the molecule without disorder are included in the discussion and in Table S11.†

Scheme 4 Syntheses of manganese(i) germyl dinitrogen complexes $[(dmpe)_2Mn(GeHR_2)(N_2)]$ (5a: R = Ph, 5b: R = Et).

to 5a–b after three days in the dark. Relative to the rich dinitrogen chemistry 56 of other d^6 transition metals such as Mo(0), 57 Fe(II), 58 and Re(I), 59 far fewer Mn(I)– N_2 complexes have been reported (see Scheme S1† and associated text). $^{54,60-75}$

In solution, a single set of NMR environments was observed for initially formed 5a and 5b (Table 1), consistent with a low symmetry cis isomer (featuring four distinct 31P NMR environments). However, the diphenyl derivative [(dmpe)₂Mn(GeHPh₂) (N_2) (5a) slowly isomerized to a higher symmetry trans isomer, affording a cis: trans ratio of ~3:1 after 3 days at room temperature in the dark (i.e. over the duration of the reaction of 1a with N2), and further conversion to achieve a 3:7 ratio occurred over an additional 12 days. Significant room temperature isomerization was not observed for the diethyl derivative [(dmpe)₂Mn(GeHEt₂)(N₂)] (5b) (upon complete consumption of 1b after 3 days, only ~2% of the dinitrogen complex had isomerized to the trans isomer). However, the trans isomer became the dominant product after heating a solution of 5b under an atmosphere of N2 at 60 °C for 1 day. This indicates that for both 5a and 5b, the trans isomer is the thermodynamically favoured product. ¹H NMR spectra of 5a-b feature GeH chemical shifts ranging from 3.02 to 5.04 ppm, where the values for each isomer of the diphenylgermyl derivative 5a are 1.72–1.75 ppm higher frequency than those of **5b**, and the *cis* isomer GeH signal is shifted 0.63-0.66 ppm to higher frequency of the trans isomer in each case (Table 1).

In contrast to the *trans* isomer of the germyl isonitrile complexes $3\mathbf{a}$ – \mathbf{c} and various other previously reported *trans*-[(dmpe)₂MnRL] complexes where the equatorial array of ³¹P nuclei gave rise to a singlet, ^{27,28,31,33,54} the ³¹P{¹H} NMR signal arising from *trans*- $5\mathbf{a}$ – \mathbf{b} was a very broad singlet ($5\mathbf{a}$) or an approximately equal-intensity sextet ($5\mathbf{b}$; left of Fig. 8) consistent with coupling to ⁵⁵Mn (nat. abund. = 100%; I = 5/2). Furthermore, the *trans* isomer of [(dmpe)₂Mn(GeHEt₂)(N₂)] ($5\mathbf{b}$) afforded a quintet at -1094 ppm in the ⁵⁵Mn{¹H} NMR spectrum at ambient temperature (right of Fig. 8), indicative of a low electric field gradient at Mn.|| The manganese–phospho-

∥The 55 Mn 1 H} NMR chemical shifts for *cis*-5a, *trans*-5a, *cis*-5b and *trans*-5b increase significantly as the temperature is increased, from -812, -991, -1070, and -1168 ppm, respectively, at 223 K, to -601, -730, -906, and -982 ppm, respectively, at 370 K. Below 272 K, the quintet arising from *trans*-5b begins to broaden significantly due to quadrupolar collapse. At elevated temperature, the 55 Mn 1 H} NMR spectra of 5a-b also contain a peak arising from [(dmpe)₂MnH (=GeR₂)] (1a-b), which is in equilibrium with 5a-b due to reversible N₂ dis-

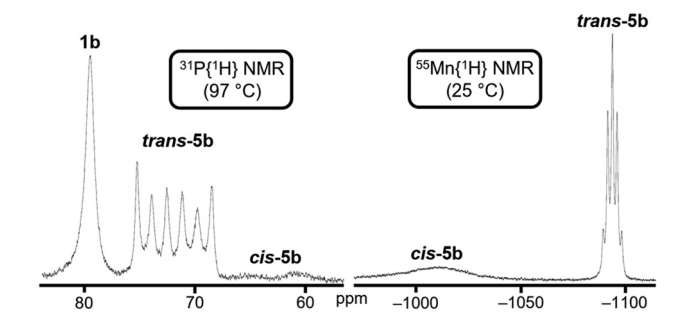


Fig. 8 31 P{ 1 H} (left, 202 MHz) and 55 Mn{ 1 H} (right, 124 MHz) NMR spectra of [(dmpe) $_{2}$ Mn(GeHEt $_{2}$)(N $_{2}$)] (5b) at 370 and 298 K, respectively (d_{8} -toluene, N $_{2}$ atmosphere), showing the sextet or quintet arising from the *trans* isomer due to 31 P $^{-55}$ Mn coupling, along with peaks arising from the *cis* isomer and from (left only) trans-[(dmpe) $_{2}$ MnH(=GeEt $_{2}$)] (1b; formed due to reversible N $_{2}$ dissociation from 5b at elevated temperature). The 31 P{ 1 H} NMR spectrum was obtained at elevated temperature to reduce the extent of quadrupolar collapse for the trans-5b signal (note that signals for cis-5b, which are broadened at this temperature, are sharp singlets at low temperature as shown in Fig. S143 † due to complete quadrupolar collapse of coupling to 55 Mn and/or slowing of a fluxional process which renders the 31 P atoms equivalent at high temperature).

rous coupling constant (${}^{1}J_{^{31}P,^{55}Mn}$) of 275 Hz in *trans*-5b is similar to those in previously reported alkyl tetracarbonyl manganese(i) complexes bearing a triphenylphosphine coligand (208–298 Hz).^{76,77} By contrast, *trans*-5a and *cis*-5a-b gave rise to broad singlets in the ${}^{55}Mn\{{}^{1}H\}$ NMR spectrum (Table 1), even upon heating to 97 °C.

Chemical shifts in ⁵⁵Mn NMR spectroscopy (δ_{55} Mn) vary widely for Mn(1) complexes.⁷⁸ For example, the trifluorophosphine complex [(F₃P)₅MnH]⁷⁹ gave rise to a ⁵⁵Mn NMR signal at -2953 ppm, compared with +1077 ppm for [CpMn(η^6 -cycloheptatriene)].80 In this work, the 55Mn chemical shifts for the cis and trans isomers of 5a-b (-718 to -1094 ppm) fall near the centre of this range. The 55Mn NMR signal for the diphenylgermyl derivative (5a) is 245-293 ppm more positive than the diethylgermyl derivative (5b), consistent with the trend previously noted for $[(R_3Sn)Mn(CO)_5]$, where δ_{55Mn} for the triphenylstannyl derivative is 50 ppm more positive than for the trimethylstannyl derivative. 81 The significant difference (79–127 ppm) in 55Mn chemical shifts arising from cis and trans isomers in 5a-b highlights the sensitivity of the 55Mn nucleus to its electronic environment; similarly 55Mn chemical shifts of -920 and -637 ppm have been reported for trans and cis isomers, respectively, of [ClMn(TeMe)₂(CO)₃], ⁸² and δ_{55Mn} differences of up to 237 ppm have been reported for various diastereomers of manganese(1) carbonyl halide complexes bearing bidentate chalcogenoether ligands. 82-85

Solutions of 5a-b in C_6D_6 are stable for days under an atmosphere of N_2 . However, in the absence of N_2 , these solutions

sociation. At 370 K, the 55 Mn $\{^{1}$ H $\}$ NMR signals arising from ${\bf 1a-b}$ are broad singlets at -1107 ppm for ${\bf 1a}$ and -1226 ppm for ${\bf 1b}$ (at 298 K, the signals are shifted to -1176 and -1303 ppm, respectively).

Paper **Dalton Transactions**

Table 1 Selected NMR spectroscopic data for dinitrogen complexes [(dmpe)₂Mn(GeHR₂)(N₂)] (5a: R = Ph, 5b: R = Et) and [(dmpe)₂Mn(SiHPh₂)(N₂)] (6). T = 298 K; δ and J are in ppm and Hz, respectively; the solvent is C_6D_6 unless otherwise specified; the ¹H NMR chemical shift is for the EH (E = Ge or Si) signal

	cis		trans			
E/R	$\delta(^{1}\mathrm{H})_{\mathrm{EH}}/^{1}J_{\mathrm{Si,H}}$	$\delta(^{31}\text{P})$	$\delta(^{55}Mn)$	$\delta(^{1}\mathrm{H})_{\mathrm{EH}}/^{1}J_{\mathrm{Si,H}}$	$\delta(^{31}P)$	$\delta(^{55}\mathrm{Mn})/^{1}J_{\mathrm{P,Mn}}$
Ge/Ph (5a) Ge/Et (5b) Si/Ph (6)	5.40 3.65 5.53/141 Hz	72.0, 69.3, 68.7, 58.7 75.5, 71.4, 65.4, 60.6 71.8, 68.5, 64.1, 58.7	-718^{a} -1011^{a} -973	4.74 3.02 4.82/140 Hz	70.6 72.3 70.8	-845^a $-1094/275 \text{ Hz}^a$ $-1098/270 \text{ Hz}$

^a ⁵⁵Mn $\{^1$ H $\}$ data for **5a-b** was obtained in d_8 -toluene.

suffered from slow dinitrogen loss to re-form the germylenehydride starting materials 1a-b. This process occurred more rapidly for 5a than 5b; ~8% conversion back to germylenehydride was observed in a sealed J-young tube under argon after 6 hours or 2 days in the dark, respectively. Dissociation of N₂ could also be promoted by exposure to light; 86-89 after 6 hours under a medium pressure mercury vapour lamp, a sealed solution of 5b in a J-young tube converted to a 1.7:1 mixture of 1b and 5b, accompanied by a small amount of decomposition to unidentified species.

Complexes 5a-b were isolated in 54-58% yield as yellow solids by removal of solvent in vacuo in the dark (5a-b are stable in vacuo for short periods of time in the absence of light) followed by recrystallization at −30 °C under argon. Analytical purity was confirmed by combustion elemental analysis (EA) and 2D powder X-ray diffraction (PXRD), and no germylene-hydride starting material was detected by IR spectroscopy (Nujol mull). Diffractograms of the bulk solids indicated that 5a was isolated as an approximate 1:3 ratio of the cis and trans isomers, whereas 5b was isolated almost exclusively as the cis isomer. In the solid state, 5a-b proved to be reasonably stable to dinitrogen loss when kept under an argon atmosphere. For example, no decomposition was observed for 5b after 2 years in a sealed vial at −30 °C as measured by PXRD and EA.

X-ray crystal structures were obtained for both the cis and trans isomers of 5a and 5b (Fig. 9 and S169;† Table 2). These complexes are octahedral with end-on terminal dinitrogen ligands, and (in all cases except trans-5a) the hydrogen atom on Ge was located from the difference map and refined isotropically. The manganese-germanium distances of 2.4795(6)-2.538(9) Å are at the higher end of the range previously reported for neutral manganese(1) germyl complexes (2.37-2.53 Å), so and are similar to those in the isonitrile complexes 3a-b (2.475(1)-2.528(1) Å). The Mn-N distances are somewhat longer in the cis isomers (1.841(2) and 1.822(2) Å) than the trans isomers (1.806(2) and 1.79(2) Å), but the N-N distances (1.120(4)-1.139(3) Å) in all four complexes are equal within 3 standard deviations. To the best of our knowledge, the only other crystallographically characterized examples of neutral Mn(1) complexes containing a terminal dinitrogen ligand are the cymantrene derivative [CpMn(CO)₂(N₂)]⁹⁰ (Mn- $N = 1.8418(4) \text{ Å}; N-N = 1.1144(1) \text{ Å})^{91}$ and the octahedral tetraphosphine hydride complex $trans-[(dmpe)_2MnH(N_2)]$ (Mn-N =

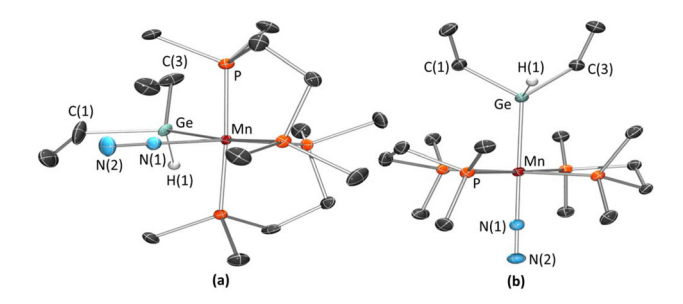


Fig. 9 X-ray crystal structures of (a) cis-[(dmpe)₂Mn(GeHEt₂)(N₂)] (cis-5b) and (b) trans-[(dmpe)₂Mn(GeHEt₂)(N₂)] (trans-5b), with ellipsoids at 50% probability. Most hydrogen atoms have been omitted for clarity, with the exception of those on Ge which were located from the difference map and refined isotropically. For cis-5b, the dmpe ligands are disordered over two positions, and only the dominant position (81.0(2)%) is shown.

1.817(5) Å; N-N = 1.127(7) Å), 54 which feature similar Mn-N and N-N distances to those in 5a-b.

IR spectroscopy (Nujol mull) was employed as a more sensitive tool to investigate differences in Mn-N2 bonding, and peaks were assigned to cis or trans isomers based on relative peak intensity (compared to expected ratios derived from PXRD). IR spectra of 5a-b included $\nu(N=N)$ stretches at 2010, 1973, 1989, and 1968 cm⁻¹ (calcd 2045, 2026, 2040, and 2018 cm $^{-1}$) for *cis-5a*, *trans-5a*, *cis-5b*, and *trans-5b*, respectively.** These data point to increased π -backdonation to N₂ in the trans complexes. The N-N stretches for both isomers of 5a-b are lower than in previously reported cyclopentadienylcontaining (2078-2169 cm⁻¹)^{64,66,90,92} and (2146-2167 cm⁻¹)^{73,74} manganese(I) complexes with terminal end-on N2 ligands. However, they are slightly higher than in $[(dmpe)_2MnH(\kappa^1-N_2)] (\nu_{N=N} = 1947 \text{ cm}^{-1}).^{54} \text{ For broader com-}$ parison, the range of $\nu(N \equiv N)$ values for end-on transition

^{**}IR spectroscopy $\nu_{N \equiv N}$ peaks for the two isomers of 5b overlap, and values reported here were obtained by peak fitting using Gaussian peak shapes and a quadratic baseline correction, which resulted in the lowest standard error and F statistic relative to alternative peak fitting methods using any combination of Gaussian, Voigt, or Gaussian/Lorentzian peak shapes, and zero, constant, linear, or quadratic background corrections (in all cases, $\nu_{N=N}$ ranged from 1988-1989 cm⁻¹ for the cis isomer and 1959-1968 cm⁻¹ for the trans isomer).

Dalton Transactions

Table 2 Selected X-ray crystallographic (and DFT calculated) bond metrics (Å or °) {and Mayer bond orders} for dinitrogen complexes [(dmpe)₂Mn $(GeHR_2)(N_2)] (5a-b)$

	cis				trans					
R	Mn-Ge	Mn-N	N = N	Ge-Mn- N	Mn-N-N	Mn-Ge	Mn-N	N = N	Ge-Mn-N	Mn-N-N
Ph (5 a) ^a	2.4867(8) (2.51) {0.81}	1.841(2) (1.80) {1.01}	1.120(4) (1.14) {2.47}	85.95(7) (86.3)	176.2(2) (176.4)	2.538(9), 2.51 (1) (2.51) {0.87}	1.79(2) (1.79) {1.11}	1.14(3) (1.14) {2.45}	165.0(8), 169.7(8) (175.9)	177(2) (179.6)
Et (5b)	2.4795(6) (2.50) {0.80}	1.822(2) (1.80) {1.04}	1.124(3) (1.14) {2.48}	86.65(5) (86.6)	178.8(2) (178.2)	2.5089(9) (2.51) {0.86}	1.806(2) (1.79) {1.12}	1.139(3) (1.14) {2.43}	177.58(6) (177.4)	179.4(2) (178.9)

^a For *trans*-5a, two sets of values are provided for some bond metrics due to a 2-part disorder of the germyl ligand.

metal dinitrogen complexes typically spans from 2250 to 1800 cm⁻¹ (cf. 2330 cm⁻¹ for free N₂).⁵⁶

DFT calculations (ADF/AMS, gas phase, all-electron, TZ2P, PBE, ZORA, D3-BJ) were carried out to further probe the nature of Mn-N₂ bonding in 5a-b. Geometry optimization of both the cis and trans isomers of 5a-b afforded structures with Mn-Ge, Mn-N, and N-N distances within 0.04 Å of the crystallographically determined values, along with Ge-Mn-N and Mn-N-N angles within three standard deviations of the XRD metrics (with the exception of Ge-Mn-N in trans-5a, which involved a disordered germyl ligand in the X-ray crystal structure).

Mayer bond orders for the Mn-N and N≡N bonds in the trans isomers are 0.08-0.10 higher and 0.02-0.05 lower, respectively, than in the cis isomers (Table 2), indicative of increased π -backdonation in the former (*trans* isomers). This is consistent with the trend indicated by N-N stretching frequencies (vide supra), which are mirrored by the DFT calculated N≡N stretching frequencies which are 19-22 cm⁻¹ lower for the trans isomers of 5a-b.

Bonding between the N₂ ligands and (dmpe)₂Mn(GeHR₂) fragments was further investigated via fragment interaction calculations using the energy decomposition analysis (EDA)⁹³ method of Ziegler and Rauk (Table 3). This approach affords an overall interaction energy, $\Delta E_{\rm int}$, which is divided into five components, as shown in eqn (1). 94,95 In this analysis, $\Delta E_{\rm elec}$ represents the electrostatic interaction energy (calculated using frozen charge distributions for both fragments), ΔE_{Pauli} corresponds to Pauli repulsion, $\Delta E_{\rm orb}$ is the orbital interaction energy (this term includes all contributions resulting from intrafragment polarization), ΔE_{disp} is the dispersion interaction energy, and ΔE_{prep} is the energy needed to bring the fragments from their optimum geometries to their geometries in the unfragmented complex.

$$\Delta E_{\rm int} = \Delta E_{\rm elec} + \Delta E_{\rm Pauli} + \Delta E_{\rm orb} + \Delta E_{\rm disp} + \Delta E_{\rm prep} \tag{1}$$

Overall interaction energies for N₂ coordination are -117 (5a) and -149 (5b) kJ mol⁻¹ for the *cis* isomers and -163 (5a) and -173 (5b) kJ mol⁻¹ for the trans isomers. Stronger N₂ bonding to manganese in the trans isomers is driven by stronger electrostatic and orbital contributions ($\Delta E_{\rm elec}$ and $\Delta E_{\rm orb}$ are more negative by 17-19 and 31-32 kJ mol⁻¹, respectively), partially offset by increased Pauli repulsion (ΔE_{Pauli} is more positive by 30-32 kJ mol⁻¹). The less negative $\Delta E_{\rm int}$ for the Mn-N₂ bond in cis-5a relative to cis-5b is driven primarily by a higher preparation energy for the (dmpe)₂Mn(GeHPh₂) fragment. This

Table 3 Fragment interaction calculation data for the cis and trans isomers of 5a-b {(dmpe)₂Mn(GeHR₂) + N₂}. All energies are in kJ mol⁻¹, ΔE_{int} values are BSSE-corrected, and for ETS-NOCV data, values in parentheses are a percentage of ΔE_{orb} . Hirsh = fragment Hirshfeld charge, [M] = (dmpe)₂Mn(GeHR₂)

	GeHR_2	<i>cis</i> -5a GeHPh ₂	trans-5a	$m{\textit{cis-}5b}$ GeHEt $_2$	trans-5b
EDA	$\Delta E_{ m int}$	-117	-163	-149	-173
	$\Delta E_{ m elec}$	-321	-338	-320	-339
	$\Delta E_{ m orb}$	-391	-422	-395	-427
	$\Delta E_{ m Pauli}$	545	575	540	572
	$\Delta E_{ m disp}$	-15	-14	-14	-14
	$\Delta E_{ m prep}$	57	28	32	26
	BSSE	9	9	9	9
Hirsh	[M]	0.29	0.34	0.31	0.35
	N_2	-0.29	-0.34	-0.31	-0.35
ETS-NOCV	ΔE_{α}	-118 (30%)	-119 (28%)	-119 (30%)	-114 (27%)
	$\Delta E_{\pi(1)}$	-129 (33%)	-138 (33%)	-131 (33%)	-142 (33%)
	$\Delta E_{\pi(2)}$	-116 (30%)	-133 (32%)	-119 (30%)	-139 (32%)
	Other	-28 (7%)	-32 (7%)	-27 (7%) [*]	-32 (8%)

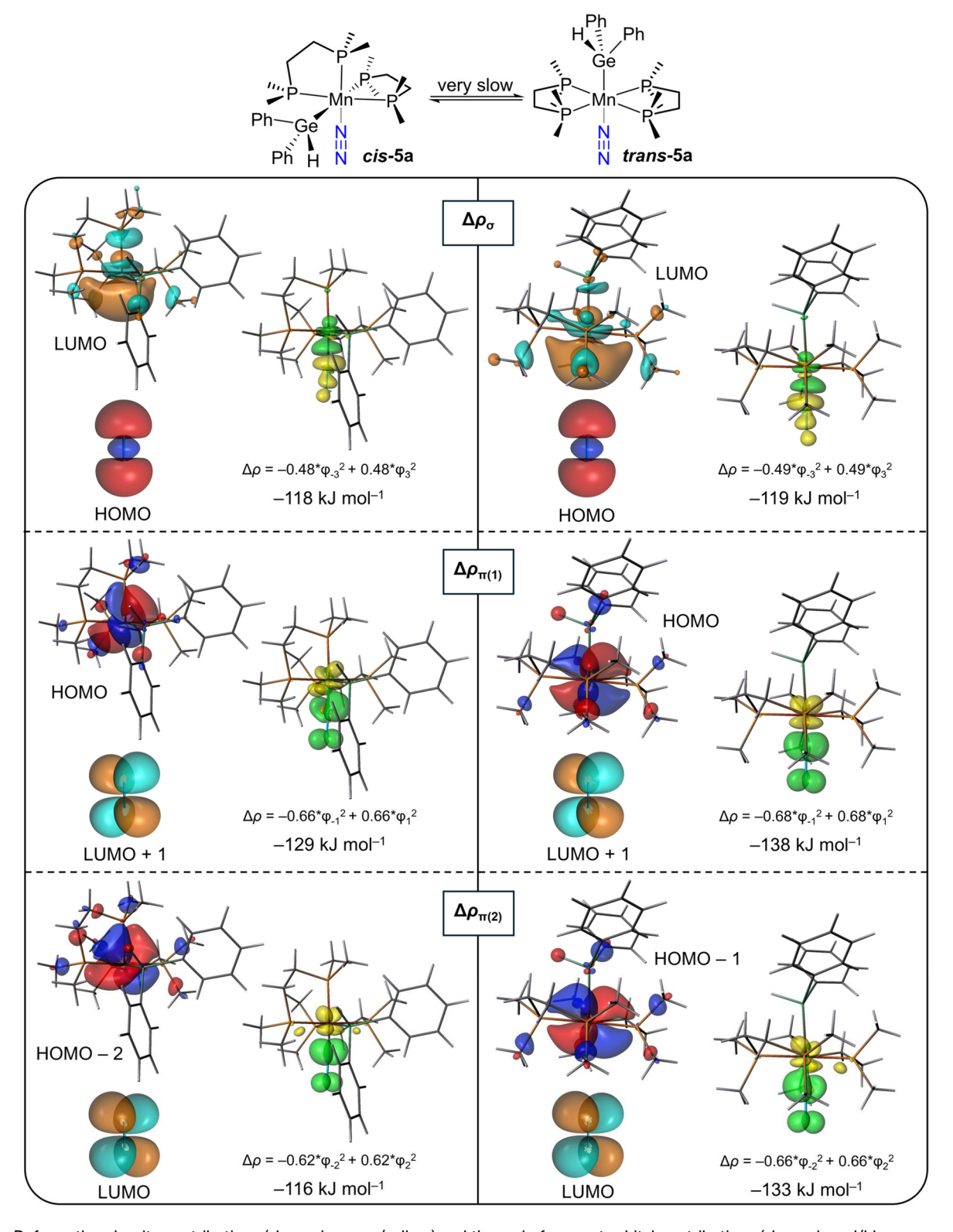


Fig. 10 Deformation density contributions (shown in green/yellow) and the main fragment orbital contributions (shown in red/blue or orange/turquoise) to bonding between a (dmpe) $_2$ Mn(GeHPh $_2$) fragment and an N $_2$ fragment in the cis- (left) and trans- (right) isomers of [(dmpe) $_2$ Mn(GeHPh $_2$) (N $_2$)] (5a). Three major interactions were observed ($\Delta\rho_{\sigma}$, $\Delta\rho_{\pi(1)}$ and $\Delta\rho_{\pi(2)}$). Deformation density isosurfaces (set to 0.003) correspond to increased (green) and decreased (yellow) electron density relative to the non-interacting fragments. Orbital isosurfaces are set to 0.03.

Dalton Transactions Paper

is due to stabilization of the geometry optimized fragment through a γ -hydride interaction involving an *ortho* C–H bond of a phenyl substituent on germanium (illustrated by a Mn···H bond distance of 1.91 Å and a Mayer bond order of 0.24; Fig. S176†).

The deformation density $(\Delta \rho)$ associated with the orbital interaction component ($\Delta E_{\rm orb}$) from fragment interaction calculations was further divided using the Extended Transition State and Natural Orbitals for Chemical Valence (ETS-NOCV) method (Table 3), affording a textbook example of end-on N₂ bonding to a transition metal. Deformation density isosurfaces and the main fragment orbital contributors for the two isomers of 5a are shown in Fig. 10 (similar figures for 5b, and the NOCVs associated with each ETS-NOCV contribution, are shown in Fig. S179-182†). In each case, three contributions of similar energy (27–33% of $\Delta E_{\rm orb}$ in all cases) were elucidated. One of these $(\Delta \rho_{\sigma})$ involves σ -donation from the HOMO of dinitrogen to the LUMO of the (dmpe)2Mn(GeHR2) fragment, whereas the other two contributions $(\Delta \rho_{\pi(1)})$ and $\Delta \rho_{\pi(2)}$ involve orthogonal π-backdonation from occupied manganese d orbitals to the vacant π^* orbitals of dinitrogen. The relative energies of these σ -donation and π -backdonation contributions are similar to those reported for other end-on N₂ complexes. 96-100

The aforementioned differences in the magnitude of $\Delta E_{\rm orb}$ between the *cis* and *trans* isomers of **5a-b** is driven exclusively by the two π interactions, which are stronger (by 7–17 kJ mol⁻¹) in the *trans* isomers. More negative Hirshfeld charges on the N₂ fragment (from fragment interaction calculations) in the *trans* isomers (–0.34 to –0.35, *versus* –0.29 to –0.31 for the *cis* isomers; Table 3) also indicate an increase in charge transfer from the (dmpe)₂Mn(GeHR₂) fragment to N₂, consistent with increased π -backdonation in the *trans* isomers.

Reaction of N₂ with [(dmpe)₂MnH(=SiPh₂)]

Given that the germylene-hydride complexes (1a-b) reacted with N_2 , we were interested to probe whether a silylene-hydride analogue would engage in analogous reactivity. Indeed, [(dmpe)₂MnH(=SiPh₂)] (which exists in solution as an equilibrium mixture of the *cis* and *trans* isomers)³¹ also reacts with dinitrogen to afford complexes tentatively identified by NMR spectroscopy as *cis* and *trans* isomers of the silyl dinitrogen complex [(dmpe)₂Mn(SiHPh₂)(N₂)] (6); Scheme 5. This reactivity reflects that previously reported for another d^6 silylene-

Scheme 5 Synthesis ($in \ situ$) of the manganese(i) silyl dinitrogen complex [(dmpe)₂Mn(SiHPh₂)(N₂)] (**6**) as a mixture of the cis and trans isomers. The starting material [(dmpe)₂MnH(\Longrightarrow SiPh₂)] exists as a mixture of the trans (minor) and cis (major) isomers; only one isomer is shown.

hydride complex, [(Cp*)(ⁱPr₂MeP)FeH(=SiHTrip)], which reversibly coordinates N₂. ¹⁰¹

Unfortunately, the synthesis of the silylene-hydride starting material affords an inseparable mixture of this complex with the silyl dihydride species [(dmpe)₂MnH₂(SiHPh₂)]³¹ (which does not react with N2 under mild conditions), so complex 6 was generated as a mixture with [(dmpe)₂MnH₂(SiHPh₂)]. X-ray quality crystals of trans-6 (Fig. S170†) were obtained from this mixture, showing that trans-6 is isostructural to the germyl derivative trans-5a, including statistically equivalent Mn-N and N-N distances. The Mn-Si distances of 2.457(3)-2.469(6) Å in trans-6 are significantly elongated relative to those in the previously reported manganese(i) SiH_nR_{3-n} (n = 1-2) complexes; the primary silyl complexes [(dmpe)₂Mn(SiH₂R)(CNR')] $(R = Ph, ^nBu, R' = ^tBu, o-xylyl; 2.3552(5)-2.3618(5) Å), ^{32}$ and the phosphine complex more electron-poor tetracarbonyl $\hbox{[(OC)}_4\hbox{Mn(SiHPh}_2\hbox{)(PPh}_3\hbox{)] (2.410(1) Å).}^{102}$

Selected NMR spectroscopic data for 6 (Table 1) includes ¹H NMR SiH environments at 5.53 (*cis-6*, ${}^{1}J_{H,Si} = 141 \text{ Hz}$) and 4.82 (*trans*-6, ${}^{1}J_{H,Si}$ = 140 Hz and ${}^{3}J_{H,P}$ = 8.6 Hz) ppm, and ${}^{29}Si$ NMR signals at 36.6 (cis-6) and 33.9 (trans-6) ppm. Similar to the NMR spectra of diethylgermyl derivative 5b, the cis isomer of 6 gave rise to multiple 31P(1H) NMR resonances and a broad singlet in the 55Mn(1H) NMR spectrum at -971 ppm, while trans-6 afforded a single ³¹P{¹H} NMR signal at 70.8 ppm which shows coupling to 55Mn in the process of quadrupolar collapse and a quintet in the 55Mn{1H} NMR spectrum at -1098 ppm ${}^{1}J_{\text{Mn,P}}$ = 270 Hz; Fig. S164 and S157†). The shift in ${}^{55}\text{Mn NMR}$ signals to more negative frequency (by 253-255 ppm) relative to those of germyl derivative 5a mirrors the previously reported trend in the tetryl-ligated manganese(I) carbonyl complexes [(R₃E)Mn(CO)₅] (R = Cl, C₆F₅, or Ph, E = Si or Ge), where δ_{55Mn} is more negative (by 40-330 ppm) in the silyl derivatives. 103 However, this trend differs from those for manganese(1) complexes which vary in the identity of a halide82-84,104,105 or chalcogenoether^{82-84,106} ligand, where more negative ⁵⁵Mn chemical shifts were observed proceeding down the group.

Summary and conclusions

Reactions of the germylene-hydride complexes [(dmpe)₂MnH (=GeR₂)] (R = Ph or Et; **1a-b**) with H₂ afforded [(dmpe)₂MnH₂(GeHR₂)] (**2a-b**) in slow equilibrium with the starting materials. This reactivity contrasts that of the silicon analogues which reacted completely to form 'silyl dihydride' complexes that are stable towards H₂ elimination. In solution, complexes **2a-b** exist as multiple isomers in rapid equilibrium, which were characterized by low temperature NMR spectroscopy. The major isomer of **2a-b** is *trans*-[(dmpe)₂MnH (HGeHR₂)] (*transHGe*-**2a-b**) featuring *trans*-disposed hydride and hydrogermane ligands, and DFT calculations indicate a higher degree of Ge–H bond oxidative addition in *transHGe*-**2a-b** compared to Si–H bond oxidative addition in the previously reported hydrosilane hydride analogues *trans*-[(dmpe)₂MnH(HSiHR₂)]. The minor isomer of **2a-b** features a

Paper Dalton Transactions

disphenoidal arrangement of the phosphine donors, and is tentatively assigned as the cis germyl dihydrogen complex cis-[(dmpe)₂Mn(GeHR₂)(H₂)] (cis-2a-b); the presence of this isomer is supported by the observation of a 1:1:1 triplet with a large (28 Hz) $J_{\rm H,D}$ coupling constant in the low-temperature ¹H{³¹P} NMR spectrum of a mixture containing partially deuterated isotopologues of 2b (where the triplet is attributed to $[(dmpe)_2Mn(GeXEt_2)(HD)] \{X = D (d_2-2b) \text{ and } H (d_1-2b)\}, \text{ both } I$ of which contain an HD ligand). However, the presence of a small amount of the germanate complex [(dmpe)₂Mn (H₂GeHR₂)] (central-2a-b), in rapid equilibrium with the cis isomer, cannot be excluded, given (a) the very similar energies of the cis and central isomers of 2a-b in DFT calculations, and (b) potential differences in the position of any cis-central equilibrium in reactions involving HD versus H₂ or D₂.

An X-ray crystal structure was obtained for transHGe-2b cocrystallized with the starting germylene complex 1b. To the best of our knowledge, this is the first crystallographically characterized example of a manganese hydrogermane complex, and more generally, transHGe-2a-b are rare examples of monometallic transition metal complexes featuring a terminal hydrogermane ligand. Reactions of 1a-b with D2 initially afforded only $[(dmpe)_2MnD_2(GeHR_2)]$ (d_2-2a-b) , suggesting that the formation of 2a-b proceeds via initial isomerization of the germylene-hydride complexes to a 5-coordinate manganese (1) germyl intermediate [(dmpe)₂Mn(GeHR₂)] (A). This intermediate was trapped by reacting [(dmpe)₂MnH(=GePh₂)] (1a) with isonitriles to afford the germyl isonitrile complexes [(dmpe)₂Mn(GeHPh₂)(CNR)] (3a-c). These complexes were formed as mixtures of cis and trans isomers, and X-ray crystal structures were obtained for either isomer depending on the isonitrile used.

Germylene-hydride complexes 1a-b also reacted slowly with dinitrogen to afford the manganese(I) germyl dinitrogen complexes [(dmpe)₂Mn(GeHR₂)(N₂)] (5a-b). Complexes 5a-b were initially formed as cis isomers, but the trans isomer became dominant over time in solution (at room temperature or with mild heating). The N_2 ligands in 5a-b are labile in solution, but the complexes are reasonably stable in the solid state. X-ray crystal structures were obtained for both isomers of 5a and 5b, providing rare examples of crystallographically characterized manganese(1) terminal N2 complexes. The silylene complex [(dmpe)₂MnH(=SiPh₂)] was also shown to react with N₂ to form the silyl dinitrogen derivative [(dmpe)₂Mn(SiHPh₂) (N_2) (6) as a mixture of *cis* and *trans* isomers.

Unusually, NMR spectra of trans-5b and trans-6 showed 1-bond coupling between ^{31}P (100% abundance, I = 1/2) and ⁵⁵Mn (100% abundance; I = 5/2), resulting in an approximate 1:1:1:1:1:1 sextet in the ³¹P{¹H} NMR spectra (at elevated temperature) and a 1:4:6:4:1 quintet in the ⁵⁵Mn{¹H} NMR spectra. Such coupling has not been observed in other $[(dmpe)_2MnXL]$ (X = an anionic ligand; L = a neutral ligand) complexes. Bonding between Mn and N2 was studied through XRD, IR spectroscopy, and DFT calculations (including ETS-NOCV analysis), revealing stronger N2 coordination in the trans isomers. This results from larger electrostatic and orbital

contributions ($\Delta E_{\rm elec}$ and $\Delta E_{\rm orb}$) to bonding, partly offset by increased Pauli repulsion (ΔE_{Pauli}), where the larger ΔE_{orb} stems from enhanced π -backdonation.

Experimental

General methods

An argon-filled MBraun UNIlab glove box equipped with a -30 °C freezer was employed for the manipulation and storage of all oxygen- and moisture-sensitive compounds. Air-sensitive preparative reactions were performed on a double-manifold high-vacuum line equipped with a two stage Welch 1402 beltdrive vacuum pump (ultimate pressure 1×10^{-4} Torr) using standard techniques. 107 The vacuum was measured periodically using a Kurt J. Lesker 275i convection enhanced Pirani gauge. Residual oxygen and moisture was removed from the argon stream by passage through an Oxisorb-W scrubber from Matheson Gas Products.

Benzene was purchased from Sigma-Aldrich, hexanes and toluene were purchased from Caledon, and deuterated solvents were purchased from ACP Chemicals. Benzene, hexanes, and toluene were initially dried and distilled at atmospheric pressure from sodium/benzophenone (first two) or sodium (toluene). All solvents were stored over an appropriate drying agent (benzene, toluene, d_8 -toluene, $C_6D_6 = Na/Ph_2CO$; hexanes = Na/Ph₂CO/tetraglyme) and introduced to reactions or solvent storage flasks via vacuum transfer with condensation at −78 °C.

Cl₂GePh₂, Cl₂GeEt₂, H₂SiPh₂, dmpe, 1,4-dioxane, ethylmagnesium chloride solution (2.0 M in diethyl ether), D2, tert-butyl isonitrile, o-xylyl isonitrile, and n-butyl isonitrile were purchased from Sigma-Aldrich. Manganese dichloride was purchased from Strem Chemicals. $[(dmpe)_2MnH(=GePh_2)](1a)_1^{29}$ $[(dmpe)_2MnH(=GeEt_2)]$ (1b),²⁹ and $[(dmpe)_2MnH(=SiPh_2)]^{31}$ were prepared according to literature procedures, as were reagents used in their preparation; $[(dmpe)_2MnH(C_2H_4)]$, ^{27,28} H₂GePh₂, ¹⁰⁸ and H₂GeEt₂. ²⁹ Argon, H₂, and N₂ were purchased from PraxAir.

NMR spectroscopy was performed on Bruker AV-500 and AV-600 spectrometers. Spectra were obtained at 298 K unless otherwise indicated. ¹H NMR spectra were referenced relative to SiMe₄ through a resonance of the protio impurity of the solvent: C_6D_6 (δ 7.16 ppm) and d_8 -toluene (δ 2.08, 6.97, 7.01, and 7.09 ppm; at lower or higher temperatures the peak at 2.08 ppm was used). 13C NMR spectra were referenced relative to SiMe₄ through a resonance of the solvent: C_6D_6 (δ 128.06 ppm) and d_8 -toluene (δ 20.43, 125.13, 127.96, 128.87, and 137.48 ppm; at lower temperatures the peak at 20.43 ppm was used). ²H NMR spectra were referenced through a resonance of the solvent C_6D_6 (δ 7.16 ppm) and the CD_3 peak in d_8 toluene (δ 2.08 ppm). The ²⁹Si, ³¹P, and ⁵⁵Mn NMR spectra were referenced to SiMe₄ (1 vol% in CDCl₃; Ξ = 19.867187%), 85% aqueous H_3PO_4 ($\Xi = 40.480742\%$), and conc. KMnO_{4(aq)} $(\Xi = 24.789218\%)$, respectively, by indirect referencing from a ¹H NMR spectrum. ¹⁰⁹ NMR chemical shift abbreviations: s =

singlet, d = doublet, t = triplet, q = quartet, quin. = quintet, m = multiplet, app. = apparent, br. = broad.

Combustion elemental analyses were performed at the University of Calgary.

IR spectroscopy was performed in a nujol mull sandwiched between CaF₂ plates using a ThermoScientific Nicolet iS5 spectrometer on transmission mode. Spectra collection and viewing was done using OMNIC.

Single-crystal X-ray crystallographic analyses were performed on crystals coated in Paratone oil and mounted on a STOE IPDS II diffractometer with an image plate detector or a Bruker Dual Source D8 Venture diffractometer using the IuS 3.0 Mo source at 70 W with a HELIOS Mo focusing optic (ELM33) in the McMaster Analytical X-Ray (MAX) Diffraction Facility. A semi-empirical absorption correction was applied using redundant and symmetry related data. Raw data was processed using XPREP (as part of the APEX4 v2022.10-0 software), and solved by intrinsic (SHELXT)¹¹⁰ methods. Structures were completed by difference Fourier synthesis and refined with full-matrix leastsquares procedures based on F^2 . In all cases, non-hydrogen atoms were refined anisotropically and hydrogen atoms were generated in ideal positions and then updated with each cycle of refinement (with the exception of hydrogen atoms on Ge and Mn, which were located from the difference map and refined isotropically). Refinement was performed with SHELXL¹¹¹ in Olex2.¹¹²

2D powder X-ray diffraction was performed on a Bruker D8 Discover diffractometer equipped with a Vantec 500 area detector and a focused Cu source with K α radiation ($\lambda = 1.54056 \text{ Å}$) operated at 40 kV and 40 mA, or a Bruker D8 Venture diffractometer equipped with a PHOTON CMOS (complementary metal oxide semiconductor) area detector and a Incoatec IµS Cu source with K α radiation ($\lambda = 1.54184$ Å) operated at 50 kV and 1.10 mA. The samples were packed in a 0.5 mm o.d. special glass (SG; wall thickness 0.01 mm) capillary tube for X-ray diffraction (purchased from Charles Supper Co.) and sealed by inverting to submerge the open end in a pool of Apiezon H-grease within the glovebox. The powder diffractograms were generated using Gadds and/or Diffrac.eva. Rietveld refinement (PV_TCHZ peak types between 5.5° and 35°, LP factor of 23.7, 6th order PO spherical harmonics for preferred orientation, and a Chebychev order 9 background) was performed using Topas.

All prepared complexes are air sensitive, and their products upon reaction with air are malodorous. Therefore, unless otherwise indicated, all syntheses were conducted under an atmosphere of argon.

DFT calculations

All calculated structures were fully optimized with the ADF/AMS DFT package (SCM, version 2020.102 for 2a-b or 2024.102 for 5a-b). 113,114 For 2a-b, energy minima were located for four (transHGe isomer) or three (cis and central isomers) rotamers, and only data from the minima leading to the lowest Gibbs free energy of formation at 176 K is discussed. Calculations were conducted in the gas phase within the generalized gradient approximation (GGA) using the 1996

Perdew–Burke–Ernzerhof exchange and correlation functional (PBE), 115 the scalar zeroth-order regular approximation (ZORA) for relativistic effects, and Grimme's DFT-D3-BJ dispersion correction. 121,122 Geometry optimizations were conducted using all-electron triple- ζ basis sets with two polarization functions (TZ2P), fine integration grids (Becke^{123,124} verygood), and stricter-than-default convergence criteria (gradients = 0.0001, step = 0.002). Calculations were restricted.

Visualization of the computational results was performed using the ADF/AMS-GUI (SCM) or Biovia Discovery Studio Visualizer. Orbitals and deformation densities were generated with a fine grid using the densf auxiliary program.

Analytical frequency calculations^{125–127} were conducted on all geometry optimized structures (including geometry optimized fragments) to ensure that the geometry optimization led to an energy minimum.

Bonding was analyzed in more detail using a fragment approach (energy decomposition analysis 128,129 with ETS-NOCV analysis $^{130-133}$) that considered the interaction of neutral (dmpe)₂Mn(GeHR₂) fragments with neutral N₂ ligands. Fragments were generated from the TZ2P geometry optimized structures of each complex, geometries were frozen, and single-point calculations (as well as the EDA/ETS-NOCV calculations) were conducted using the same parameters as for the geometry optimizations. Preparation energies ($\Delta E_{\rm prep}$) were obtained for all fragments by allowing the fragments to adopt equilibrium geometries (using the same method previously described for geometry optimization). Basis set superposition errors (BSSEs) were calculated through the use of ghost atoms with no nuclear charge and no electrons to contribute to the molecule (using the molecular fragments method).

Reaction of [(dmpe)₂MnH(=GePh₂)] (1a) with H₂ to afford mixtures containing 1a, H2, and [(dmpe)2MnH2(GeHPh2)] (2a). Approx. 10 mg of [(dmpe)₂MnH(=GePh₂)] (1a) was dissolved in approx. 0.6 mL of C_6D_6 or d_8 -toluene, and the solution placed in a J-young NMR tube. The mixture was freeze/pump/ thawed three times, and placed under 1 atm of H_2 at -95 °C, sealed, and warmed to room temperature. This reaction was monitored over time in situ by NMR spectroscopy and had reached equilibrium within 3 days with 87% conversion to 2a, at which time the solution had turned light orange. ¹H NMR (C₆D₆, 600 MHz, 298 K): δ 7.97 (d of d, 4H, ${}^{3}J_{H,H}$ 7.9 Hz, ${}^{4}J_{H,H}$ 1.4 Hz, o-Ph), 7.22 (t, 4H, ³J_{H,H} 7.4 Hz, m-Ph), 7.11 (t of t, 2H, ${}^{3}J_{\rm H,H}$ 7.3 Hz, ${}^{4}J_{\rm H,H}$ 1.4 Hz, p-Ph), 5.90 (m, 1H, GeH), 1.32 (m, 8H, PCH₂), 1.18 (br. s, 24H, PCH₃), -11.09 (br. m, 2H, MnH). ¹H NMR (d_8 -toluene, 500 MHz, 298 K): δ 7.85 (d of d, 4H, $^3J_{\rm H,H}$ 6.5 Hz, ⁴J_{H,H} 1.3 Hz, o-Ph), 7.14 (t, 4H, ³J_{H,H} 7.3 Hz, m-Ph), 7.05 (t of t, 2H, ${}^{3}J_{H,H}$ 7.3 Hz, ${}^{4}J_{H,H}$ 1.9 Hz, p-Ph), 5.78 (m, 1H, Ge<u>H</u>), 1.30 (m, 8H, PCH₂), 1.15 (br. s, 24H, PCH₃), -11.13 (br. m, 2H, Mn*H*). ¹³C{¹H} NMR (d_8 -toluene, 126 MHz, 298 K): δ 155.21 (s, i-Ph), 135.81 (s, o-Ph), 127.40 (s, m-Ph), 126.07 (s, p-Ph), 32.70 (m, PCH₂), 25.60 (m, PCH₃). ${}^{31}P{}^{1}H$ NMR (d_8 -toluene, 202 MHz, 298 K): δ 76.18 (s). transHGe-2a: ¹H NMR (d_8 **toluene**, **500 MHz**, **176 K**): δ 8.05 (d, 4H, ${}^{3}J_{H,H}$ 7.1 Hz, o-Ph), 7.27 (t, 4H, ${}^{3}J_{H,H}$ 7.2 Hz, m-Ph), 7.14 (t, 2H, ${}^{3}J_{H,H}$ 7.2 Hz, p-Ph), 6.05 (d, 1H, ${}^{2}J_{H,H}$ 15.8 Hz, GeH), 1.46, 1.21 (2 × br. s, 4H,

 PCH_2), 1.24, 0.96 (2 × s, 12H, PCH_3), -10.53 (m, 1H, MnHGe), -11.19 (quin, 1H, ${}^{2}J_{H,P}$ 57.9 Hz, MnH). ${}^{13}C\{{}^{1}H\}$ NMR (d_{8} toluene, 126 MHz, 176 K): δ 154.76 (s, i-Ph), 135.24 (s, o-Ph), 127.51 (s, m-Ph), 126.20 (s, p-Ph), 31.43 (m, PCH₂), 28.66, 21.51 $(2 \times s, PCH_3)$. ³¹P{¹H} NMR (d_8 -toluene, 202 MHz, 176 K): δ 78.14 (s). Isomers(s) of 2a with a disphenoidal arrangement of the phosphine donors (selected data): ${}^{1}H$ NMR (d_{8} -toluene, **500 MHz, 176 K)**: δ 8.32 (d, 2H, ${}^{3}J_{\text{H,H}}$ 6.9 Hz, o-Ph), 7.99 (d, 2H, $^{3}J_{H,H}$ 7.0 Hz, o-Ph), 7.42 (t, 2H, $^{3}J_{H,H}$ 7.1 Hz, m-Ph), 7.24 (t, 2H, ³J_{H,H} 7.3 Hz, m-Ph), 5.49 (m, 1H, GeH), 1.52, 1.26, 1.00, 0.81, 0.57 (5 × s, 3H, P<u>C</u>H₃), 1.39 (d, 3H, ${}^{2}J_{H,P}$ 5.6 Hz, PC<u>H</u>₃), 0.74 (d, 3H, ${}^{2}J_{H,P}$ 4.6 Hz, PC H_{3}), 0.72 (d, 3H, ${}^{2}J_{H,P}$ 4.0 Hz, PC H_{3}), -13.29 (br. s, 2H, MnH). $^{13}C\{^{1}H\}$ NMR (d_{8} -toluene, 126 MHz, **176 K)**: δ 156.67 (s, *i*-Ph), 136.67 (s, *o*-Ph), 127.09 (s, *m*-Ph), 29.94 (d, $J_{C,P}$ 20.2 Hz, PCH₃), 28.17, 25.10, 23.04, 21.18 (4 × s, PCH₃), 27.57 (d, J_{C,P} 18.5 Hz, PCH₃), 21.90 (d, J_{C,P} 10.0 Hz, PCH_3), 19.51 (d, $J_{C,P}$ 15.5 Hz, PCH_3). ³¹ $P\{^{1}H\}$ NMR (d_8 -toluene, **202 MHz, 176 K):** δ 76.11, 73.42 (2 × s, 1P), 71.22 (s, 2P).

Reaction of $[(dmpe)_2MnH(=GeEt_2)]$ (1b) with H₂ to afford mixtures containing 1b, H2, and [(dmpe)2MnH2(GeHEt2)] (2b). This was done in an analogous fashion to the reaction between 1a and H₂, using [(dmpe)₂MnH(=GeEt₂)] (1b) in place of 1a, and resulting in 73% conversion to 2b after reaching equilibrium (after 2 days), at which time the solution had turned yellow. ¹H NMR (C_6D_6 , 600 MHz, 298 K): δ 4.28 (s, 1H, GeH), 1.61 (t, 6H, ${}^{3}J_{H,H}$ 7.8 Hz, $CH_{2}CH_{3}$), 1.35 (m, 8H, PCH_{2}), 1.23 (s, 24H, PC H_3), 1.09, 1.00 (2 × m, 2H, C H_2 C H_3), -11.93 (m, 2H, MnH). ¹H NMR (d_8 -toluene, 500 MHz, 298 K): δ 4.15 (s, 1H, GeH), 1.41 (t, 6H, ³J_{H,H} 7.8 Hz, CH₂CH₃), 1.33 (m, 8H, PCH_2), 1.21 (s, 24H, PCH_3), 0.99, 0.91 (2 × m, 2H, CH_2CH_3), -12.00 (m, 2H, MnH). $^{13}C\{^{1}H\}$ NMR (d_{8} -toluene, 126 MHz, 298 K): δ 33.54 (m, PCH₂), 25.48 (s, PCH₃), 16.10 (s, CH₂CH₃), 14.59 (s, CH_2CH_3). ³¹P{¹H} NMR (d_8 -toluene, 202 MHz, 298 K): δ 75.53 (s). transHGe-2b: ¹H NMR (d_8 -toluene, 500 MHz, **176 K)**: δ 4.55 (s, GeH, 1H), 1.73 (m, 6H, CH₂CH₃), 1.52, 1.24 $(2 \times br. s, 4H, PCH_2), 1.32, 1.10 (2 \times s, PCH_3, 12H), 1.22, 1.01$ $(2 \times CH_2CH_3)$, †† -11.01 (m, 1H, MnHGe), -11.28 (quin, 1H, $_{J_{\text{H.P}}}^{2}$ 56.0 Hz, Mn*H*). $_{13}^{13}\text{C}\{^{1}\text{H}\}$ NMR (d_{8} -toluene, 126 MHz, **176 K)**: δ 32.73 (m, PCH₂), 27.52 (m, PCH₃), 22.37 (s, PCH₃), 15.23 (s, CH_2CH_3), 14.28 (s, CH_2CH_3). ³¹ $P{^1}H$ } NMR (d_8 toluene, 202 MHz, 176 K): δ 76.49 (s). Isomers(s) of 2b with a disphenoidal arrangement of the phosphine donors (selected data): ¹H NMR (d_8 -toluene, 500 MHz, 176 K): δ 3.86 (s, 1H, GeH), 2.08 (m, 3H, CH_2CH_3), 1.91, 1.28, 1.12 (3 × PCH_3), †† 1.37, 0.99, 0.95, 0.94 0.76 (5 × s, 3H, PC H_3), 1.36 (C H_2 C H_3), †† -13.85 (br. s, 2H, MnH). $^{13}C\{^{1}H\}$ NMR (d_{8} -toluene, 126 MHz, **176 K)**: δ 25.03 (d, $J_{C,P}$ 12.8 Hz, PCH₃), 22.69 (d, $J_{C,P}$ 11.8 Hz, PCH₃), 22.66 (m, PCH₃), 16.89 (s, CH₂CH₃), 16.06 (s, PCH₃). ³¹P{¹H} NMR (d_8 -toluene, 202 MHz, 176 K): δ 74.65 (s, 2P), 72.68, 71.97 ($2 \times s$, 1P).

Reactions of $[(dmpe)_2MnH(=GeR_2)]$ (R = Ph: 1a, R = Et: 1b) with D₂ to afford mixtures containing 1a or 1b, D₂, and

[(dmpe)₂MnD₂(GeHR₂)] (R = Ph: d_2 -2a, R = Et: d_2 -2b). These reactions were conducted in an analogous fashion to those described above for reactions of 1a–b with H₂ (in C₆D₆ or d_8 -toluene), but using D₂ in place of H₂. To monitor deuterium scrambling in 2a, the reaction (in C₆D₆) was heated in the J-young tube at 60 °C and periodically analysed by NMR spectroscopy at room temperature. ¹H and ³¹P{¹H} NMR spectra at 298 K in C₆D₆ of 2a–b mirror those of 1a–b, with the exception that the Mn \underline{H} ¹H NMR environment is not present and the Ge \underline{H} ¹H NMR signal shifted slightly to 5.87 (d_2 -2a) or 4.24 (d_2 -2b) ppm. [(dmpe)₂MnD₂(HGePh₂)] (d_2 -2a): ²H NMR (C₆D₆, 77 MHz, 298 K): δ –11.28 (app. t, ² $J_{D,P}$ 5.0 Hz, Mn \underline{D}). [(dmpe)₂MnD₂(HGeEt₂)] (d_2 -2b): ²H NMR (C₆D₆, 77 MHz, 298 K): δ –12.16 (quin, ² $J_{D,P}$ 4.7 Hz, Mn \underline{D}).

X-ray quality crystals of $[(dmpe)_2MnH(=GeEt_2)]$ (1b) and transHGe- $[(dmpe)_2MnH(HGeHEt_2)]$ (transHGe-2b). 11.7 mg (0.02 mmol) of $[(dmpe)_2MnH(=GeEt_2)]$ (1b) was dissolved in 0.35 mL of toluene, and the solution was placed in a 25 mL Schlenk flask, freeze/pump/thawed three times, placed under 1 atm of H_2 at -78 °C, sealed, and warmed to room temperature. The reaction mixture was then stirred for 2 days, after which the solvent was removed *in vacuo*, ~0.5 mL of hexanes was added, and the solution was placed under 1 atm of H_2 at -78 °C and sealed. Maintaining the solution at -78 °C for a few hours afforded large yellow X-ray quality crystals containing a mixture of 1b and transHGe-2b (due to disorder between two germyl groups and a germylene group in a 0.402 (3): 0.056(3): 0.542(3) ratio).

 $[(dmpe)_2Mn(GeHPh_2)(CN^tBu)]$ (3a). (a) 75.2 mg (0.13 mmol) of $[(dmpe)_2MnH(=GePh_2)]$ (1a) was dissolved in 10 mL of benzene and placed in a 50 mL storage flask. 21.4 mg (0.26 mmol) of tert-butyl isonitrile was added and the reaction mixture was stirred for 1.5 hours at room temperature in the dark. The solvent was removed in vacuo, and the resulting yellow solid was dried in vacuo for 1 hour and washed with 4 mL of hexanes. Recrystallization of the residue (which did not dissolve in hexanes) at −30 °C from a solution in toluene layered with the hexanes that had been used to wash the crude material afforded 36.0 mg (0.05 mmol, 42%) of cis-3a as X-ray quality yellow crystals. The reaction of 1a with CN^tBu affords 3a in near quantitative spectroscopic yield (as a mixture of cis and trans isomers), so the low yield is due to losses during crystallization. (b) 15.3 mg (0.03 mmol) of [(dmpe)₂MnH $(=GePh_2)$] (1a) and 4.4 mg (0.05 mmol) of tert-butyl isonitrile were dissolved in approx. 0.6 mL of C₆D₆, placed in a J-young tube, and the reaction mixture was monitored over time at room temperature by NMR spectroscopy. After 30 minutes, the reaction mixture contained cis-3a and trans-3a in a 3:1 ratio, which remained constant over 4 days. cis-3a: ¹H NMR (C₆D₆, **600 MHz, 298 K)**: δ 8.20, 8.15 (2 × d of d, 2H, ${}^{3}J_{H,H}$ 7.6 Hz, ${}^{4}J_{H,H}$ 1.0 Hz, o-Ph), 7.25, 7.22 (2 × t, 2H, ${}^{3}J_{H,H}$ 7.9 Hz, m-Ph), 7.12 (t, 1H, ${}^{3}J_{H,H}$ 7.6 Hz, p-Ph), 7.08 (t, 1H, ${}^{3}J_{H,H}$ 7.4 Hz, p-Ph), 5.45 (t of d, 1H, ${}^{3}J_{H,P}$ 8.6 and 5.2 Hz, Ge<u>H</u>), 1.80, 1.62 (2 × m, 1H, PCH_2), 1.71 (d, 3H, ${}^2J_{H,P}$ 6.7 Hz, PCH_3), 1.69 (d, 3H, ${}^2J_{H,P}$ 6.9 Hz, PCH_3), 0.94-1.49 (m, 6H, PCH_2), 1.34, 1.16 (2 × d, 3H, $^{2}J_{H,P}$ 6.6 Hz, PC \underline{H}_{3}), 1.20 (d, 3H, $^{2}J_{H,P}$ 5.9 Hz, PC \underline{H}_{3}), 1.10 (d,

^{††}This NMR environment was located using 2D NMR spectroscopy, and thus no integration and/or environment splitting information is provided.

3H, ${}^{2}J_{H,P}$ 5.8 Hz, PC H_{3}), 1.03 (s, 9H, C(C H_{3})₃), 0.97 (d, 3H, ${}^{2}J_{H,P}$ 4.6 Hz, PC H_3), 0.82 (d, 3H, ${}^2J_{H,P}$ 4.8 Hz, PC H_3). ${}^{13}C\{{}^1H\}$ NMR (C₆D₆, 151 MHz, 298 K): δ 158.29 (d, ${}^{3}J_{C,P}$ 2.6 Hz, *i*-Ph), 157.74 (d, ${}^{3}J_{CP}$ 3.4 Hz, *i*-Ph), 137.65, 137.47 (2 × s, *o*-Ph), 127.23, 127.10 (2 × s, m-Ph), 125.23, 125.20 (2 × s, p-Ph), 54.94 (s, CMe_3), 34.62 (app. t of d, J_{CP} 20.7 and 5.5 Hz, PCH_2), 33.64 (app. t of d, $J_{C,P}$ 23.3 and 7.5 Hz, PCH₂), 33.13 (app. t, $J_{C,P}$ 20.4 Hz, PCH_2), 31.46 (s, $C(CH_3)_3$), 30.62 (app. t, $J_{C,P}$ 19 Hz, PCH_2), 24.31 (d of d, J_{C,P} 14.1 and 5.2 Hz, PCH₃), 23.92 (d, J_{C,P} 12.4 Hz, PCH₃), 23.43 (d of d, $J_{C,P}$ 16.0 and 5.8 Hz, PCH₃), 23.04 (d, $J_{C,P}$ 8.0 Hz, PCH₃), 22.40 (d of d, $J_{C,P}$ 17.9 and 6.0 Hz, PCH₃), 21.73 (m, PCH₃), 21.01 (d of m, $J_{C,P}$ 20.5 Hz, PCH₃). ³¹P{¹H} NMR (C_6D_6 , 243 MHz, 298 K): δ 75.78, 56.99 (2 × s, 1P), 70.53 (s, 2P). trans-3a: 1 H NMR (C₆D₆, 500 MHz, 298 K): δ 8.00 (d, 4H, ${}^{3}J_{H,H}$ 7.1 Hz, o-Ph), 7.19 (m, m-Ph), 5.12 (quin., 1H, ${}^{3}J_{H,P}$ 7.7 Hz, GeH), 1.85, 1.44 (2 × m, 4H, PCH₂), 1.40, 1.18 (2 × s, 12H, PCH_3), 0.98 (s, 9H, $C(CH_3)_3$). $^{13}C\{^1H\}$ NMR (C_6D_6 , 126 MHz, **298 K)**: δ 158.83 (s, *i*-Ph), 137.10 (s, *o*-Ph), 127.38 (s, *m*-Ph), 125.36 (s, p-Ph), 54.55 (s, CMe₃), 32.52 (m, PCH₂), 31.36 (s, C(CH₃)₃), 21.72 (m, PCH₃). ³¹P{¹H} NMR (C₆D₆, 202 MHz, 298 K): δ 72.71 (s). Anal. found (calcd): C, 52.31 (52.28); H, 8.00 (7.87); N, 2.10 (2.08).

Monitoring of conversion for reactions of 1a with isonitriles to form $[(dmpe)_2Mn(GeHPh_2)(CNR)]$ (3b: R = o-xylyl, 3c: R = ⁿBu). $[(dmpe)_2MnH(=GePh_2)]$ (1a; for 3b 11.6 mg/0.02 mmol, and for 3c 13.3 mg/0.02 mmol) and free isonitrile (for 3b 5.2 mg/0.04 mmol of o-xylyl isontrile, and for 3c 7.0 mg/ 0.08 mmol of *n*-butyl isonitrile) were dissolved in approx. 0.6 mL of C₆D₆, placed in a J-young tube, and the reaction mixtures were monitored over time at room temperature by NMR spectroscopy. Both reactions were complete after 1 hour. cis-**3b**: 1 H NMR (C₆D₆, 600 MHz, 298 K): δ 8.07 (d of m, 2H, ${}^{3}J_{H,H}$ 7.2 Hz, o-Ph), 8.03 (d of d, 2H, ³J_{H,H} 7.8 Hz, ⁴J_{H,H} 1.2 Hz, o-Ph), 7.13 (t, 2H, ${}^{3}J_{H,H}$ 7.4 Hz, m-Ph), 7.07 (m, 2H, p-Ph), 7.06 (m, 2H, m-Ph), 6.90 (d, 2H, ${}^{3}J_{H,H}$ 7.5 Hz, xylyl-m), 6.80 (t, 1H, ${}^{3}J_{H,H}$ 7.5 Hz, xylyl-p), 5.48 (q, 1H, ${}^{3}J_{H,P}$ 6.6 Hz, Ge<u>H</u>), 2.10 (s, 6H, xylyl-C H_3), 1.72 (d, 3H, ${}^2J_{H,P}$ 7.0 Hz, PC H_3), 1.63 (d, 3H, ${}^2J_{H,P}$ 6.8 Hz, PC H_3), 1.47–1.61 (m, 2H, PC H_2), 1.51, 1.13 (2 × d, 3H, $^{2}J_{H,P}$ 6.2 Hz, PC H_{3}), 1.04–1.40 (m, 5H, PC H_{2}), 1.19 (d, 3H, $^{2}J_{H,P}$ 5.9 Hz, PC \underline{H}_3), 0.98 (d, 3H, ${}^2J_{H,P}$ 6.1 Hz, PC \underline{H}_3), 0.90, 0.80 (2 × d, 3H, ${}^{2}J_{H,P}$ 4.8 Hz, PC H_{3}), 0.88 (m, 1H, PC H_{2}). ${}^{13}C\{{}^{1}H\}$ NMR (C₆D₆, 151 MHz, 298 K): δ 156.22 (s, *i*-Ph), 155.39 (d, ${}^{3}J_{\text{C,P}}$ 4.0 Hz, *i*-Ph), 137.78, 137.19 (2 × s, *o*-Ph), 133.69 (s, xylyl- \hat{i}), 133.11 (s, xylyl-o), 128.16 (xylyl-m), †† 127.22, 127.10 (2 \times s, m-Ph), 125.41, 125.36 (2 \times s, p-Ph), 122.62 (s, xylyl-p), 33.81 (app. t, $J_{C,P}$ 19.9 Hz, PCH₂), 33.17 (m, PCH₂), 31.86 (app. t, $J_{C,P}$ 20.1 Hz, PCH₂), 23.68 (d of m, J_{C,P} 16.0 Hz, PCH₃), 22.50, 21.74, 21.05 (3 × m, PCH_3), 20.72 (s, xylyl- CH_3). ³¹ $P{^1H}$ NMR $(C_6D_6, 243 \text{ MHz}, 298 \text{ K}): \delta 70.57 \text{ (s, 2P)}, 67.94, 53.44 \text{ (2 × s, 1P)}.$ *trans*-3b: ¹H NMR (C_6D_6 , 600 MHz, 298 K): δ 7.95 (d of d, 4H, ${}^{3}J_{H,H}$ 7.7 Hz, ${}^{4}J_{H,H}$ 1.2 Hz, o-Ph), 7.18 (t, 4H, ${}^{3}J_{H,H}$ 7.3 Hz, *m*-Ph), 7.07 (m, 2H, *p*-Ph), 6.83 (d, 2H, ³J_{H,H} 7.5 Hz, xylyl-*m*), 6.69 (t, 1H, ${}^{3}J_{H,H}$ 7.5 Hz, xylyl-p), 5.27 (quin., 1H, ${}^{3}J_{H,P}$ 7.3 Hz, GeH), 2.24 (s, 6H, xylyl-C H_3), 1.71, 1.52 (2 × m, 4H, PC H_2), 1.41, 1.21 (2 × s, 12H, PC H_3). ¹³C{¹H} NMR (C₆D₆, 151 MHz, **298 K):** δ 157.67 (s, *i*-Ph), 137.32 (s, *o*-Ph), 133.81 (s, xylyl-*i*), 132.11 (s, xylyl-o), 128.68 (s, xylyl-m), 127.50 (s, m-Ph), 125.60

(s, p-Ph), 122.25 (s, xylyl-p), 32.86 (m, PCH₂), 22.49, 21.91 (2 \times m, PCH_3), 20.63 (s, xylyl- CH_3). ³¹ $P{^1H}$ NMR (C_6D_6 , 243 MHz, 298 K): δ 70.57 (s). *cis*-3c: ¹H NMR (C₆D₆, 600 MHz, 298 K): δ 8.21, 8.13 (2 × d, 2H, ${}^{3}J_{\text{H.H}}$ 7.8 Hz, o-Ph), 7.27, 7.22 (2 × t, 2H, $^{3}J_{\rm H.H}$ 7.5 Hz, *m*-Ph), 7.15 (t, 1H, $^{3}J_{\rm H,H}$ 7.5 Hz, *p*-Ph), 7.11 (t, 1H, $^{3}J_{\rm H,H}$ 7.3 Hz, p-Ph), 5.46 (app. t of d, 1H, $^{3}J_{\rm H,P}$ 8.6 and 4.7 Hz, GeH), 3.16 (m, 2H, $CH_2CH_2CH_2CH_3$), 1.75, 1.61, 140 (3 × m, 1H, PC H_2), 1.64, 1.18 (2 × d, 3H, ${}^2J_{H,P}$ 6.2 Hz, PC H_3), 1.62 (d, 3H, ${}^{2}J_{H,P}$ 6.5 Hz, PC \underline{H}_{3}), 1.39, 1.14, 1.06 (3 × d, 3H, ${}^{2}J_{H,P}$ 6.0 Hz, PCH₃), 1.21 (m, 2H, CH₂CH₂CH₂CH₃), 1.19 (m, 2H, CH₂CH₂CH₂CH₃), 1.07-1.12 (m, 3H, PCH₂), 0.92-1.05 (m, 2H, PCH_2), 0.95 (d, 3H, ${}^2J_{H,P}$ 4.7 Hz, PCH_3), 0.81 (d, 3H, ${}^2J_{H,P}$ 4.9 Hz, PC H_3), 0.79 (t, 3H, ${}^3J_{H,H}$ 7.1 Hz, CH₂CH₂CH₂CH₃). ${}^{13}C\{{}^{1}H\}$ **NMR** (C₆D₆, 151 MHz, 298 K): δ 157.61, 157.41 (2 × s, *i*-Ph), 137.63, 137.28 (2 \times s, o-Ph), 127.20, 127.13 (2 \times s, m-Ph), 125.30, 125.27 (2 \times s, p-Ph), 45.12 (s, $CH_2CH_2CH_2CH_3$), 34.22, 33.41 (2 × m, PCH₂), 33.08 (s, $CH_2CH_2CH_2CH_3$), 30.48 (app. t, $J_{\rm C.P}$ 19.3 Hz, PCH₂), 24.47, 23.01, 22.85, 21.34, 21.11, 20.95 (6 × m, PCH₃), 23.53 (d, J_{C,P} 13.2 Hz, PCH₃), 22.38 (d of d, J_{C,P} 20.3 and 5.6 Hz, PCH₃), 20.40 (s, CH₂CH₂CH₂CH₃), 13.76 (s, $CH_2CH_2CH_2CH_3$). ³¹P{¹H} NMR (C₆D₆, 243 MHz, 298 K): δ 76.11, 53.33 (2 × s, 1P), 71.59 (s, 2P). *trans*-3c (selected): 1 H **NMR** (C₆D₆, 600 MHz, 298 K): δ 7.96 (d, 4H, ${}^{3}J_{H,H}$ 7.1 Hz, o-Ph), 5.06 (quin., 1H, ${}^{3}J_{H,P}$ 15.5 Hz, GeH), 1.81, 1.43 (2 × m, 4H, PC H_2), 1.36, 1.16 (2 × s, 12H, PC H_3). ¹³C{¹H} NMR (C₆D₆, **151 MHz, 298 K):** δ 137.01 (s, o), 127.42, 125.45 (2 × s, m and p), 32.26 (m, PCH₂), 22.97, 21.30 (2 × m, PCH₃). 31 P{ 1 H} NMR $(C_6D_6, 243 \text{ MHz}, 298 \text{ K}): \delta 73.77 \text{ (s)}.$

X-ray quality crystals of *cis*-[(dmpe)₂Mn(GeHPh₂)(CNXyl)] (3b) and [(dmpe)₂MnH(CNXyl)] (4). The reaction of 1a with *o*-xylyl isonitrile was allowed to proceed to completion as described above, at which point it was heated overnight at 100 °C to afford a mixture containing *cis*-3b, *trans*-3b, and 4 in a 24:3:73 ratio. The solvent was then removed *in vacuo*, the resulting solid was extracted with hexanes, and the mother liquors were stored at -30 °C to afford X-ray quality yellow crystals of 4. The remaining solid (which did not dissolve in hexanes) was dissolved in minimal toluene, and that solution was stored at -30 °C to afford yellow crystals from which an X-ray structure of *cis*-3b was obtained.

X-ray quality crystals of trans-[(dmpe)₂Mn(GeHPh₂)(CNⁿBu)] (3c). 47.7 mg (0.08 mmol) of [(dmpe)₂MnH(\equiv GePh₂)] (1a) was dissolved in 5 mL of benzene, and the solution was transferred to a 50 mL storage flask. 25.1 mg (0.30 mmol) of n-butyl isonitrile was added, and the reaction was stirred for 1 hour at room temperature. Removal of the solvent $in\ vacuo$ afforded an orange oil which was dried $in\ vacuo$ for 1 hour at room temperature. The oil was extracted with 1.5 mL of hexanes to afford an orange solution which was stored at $-30\ ^{\circ}$ C to afford yellow crystals from which an X-ray structure of trans-3c was obtained. Recrystallization of the residue (which did not dissolve in hexanes) at $-30\ ^{\circ}$ C from toluene layered with hexanes afforded 4.7 mg (0.01 mmol) of cis-3c, in >95% purity (measured by NMR spectroscopy).

 $[(dmpe)_2Mn(GeHPh_2)(N_2)]$ (5a). 50.1 mg (0.09 mmol) of $[(dmpe)_2MnH(=GePh_2)]$ (1a) was dissolved in 5 mL of benzene

and placed in a 100 mL storage flask. The mixture was freeze/ pump/thawed three times, placed under 1 atm of N_2 at -95 °C, sealed, and warmed to room temperature. After stirring for 5 days at room temperature in the dark, the solvent was removed in vacuo. The resulting solid was recrystallized from a concentrated solution of toluene layered with a concentrated solution of hexanes at -30 °C to afford 28.4 mg (0.05 mmol, 54%) of 5a as yellow crystals. X-ray quality crystals of cis-5a were obtained by recrystallization from a concentrated solution in toluene layered with hexanes at -30 °C. X-ray quality crystals of *trans*-5a were obtained by serendipitous N2 addition to a reaction mixture formed from the combination of approx. 10 mg of 1a with H_2 in d_8 -toluene, followed by removal of the solvent in vacuo and recrystallization from toluene at -30 °C. NMR spectra were obtained under an atmosphere of N2. cis-5a: ν (N=N): 2010 cm⁻¹, ν (Ge-H): 1860 cm⁻¹ (very broad). ¹H NMR (C₆D₆, 600 MHz, 298 K): δ 8.22, 8.11 (2 × d, 2H, ${}^{3}J_{H,H}$ 7.0 Hz, o-Ph), 7.34, 7.24 (2 × t, 2H, ${}^{3}J_{H,H}$ 7.4 Hz, m-Ph), 7.17 (t, ${}^{3}J_{H,H}$ 7.7 Hz, p-Ph), ‡‡ 7.12 (t, 1H, ${}^{3}J_{H,H}$ 7.3 Hz, p-Ph), 5.40 (q, 1H, ${}^{3}J_{H,P}$ 5.4 Hz, GeH), 0.70-1.74 (m, 8H, PC H_2), 1.48 (d, 6H, ${}^2J_{H,P}$ 6.8 Hz, PC \underline{H}_3), 1.29 (PC \underline{H}_3),†† 1.09 (d, 3H, $^2J_{\rm H,P}$ 6.1 Hz, PC \underline{H}_3), 0.99 (d, 3H, ${}^{2}J_{H,P}$ 6.5 Hz, PC \underline{H}_{3}), 0.93 (d, 3H, ${}^{2}J_{H,P}$ 5.9 Hz, PC \underline{H}_{3}), 0.85 (d, 3H, ${}^{2}J_{H,P}$ 5.1 Hz, PC H_{3}), 0.53 (d, 3H, ${}^{2}J_{H,P}$ 5.3 Hz, PC H_3). ¹³C{¹H} NMR (C₆D₆, 151 MHz, 298 K): δ 154.87, 153.61 $(2 \times s, i-Ph)$, 137.80, 137.22 $(2 \times s, o-Ph)$, 127.49, 127.34 $(2 \times s, o-Ph)$ m-Ph), 125.84 (s, p-Ph), 125.73 or 125.68 (s, p-Ph),§§ 33.18, 29.30 (2 × m, PCH₂), 32.53 (app. t, $J_{C,P}$ 20.8 Hz, PCH₂), 23.09, 21.90, 21.80, 16.52 (4 × m, PCH₃), 22.64 (d of d, $J_{C,P}$ 18.5 and 5.8 Hz, PCH₃), 19.87 (d, J_{C,P} 16.8 Hz, PCH₃), 17.45 (d, J_{C,P} 18.7 Hz, PCH₃), 15.31 (d of d, $J_{C,P}$ 17.3 and 4.8 Hz, PCH₃). ³¹P{¹H} NMR (C_6D_6 , 243 MHz, 298 K): δ 71.98, 69.33, 68.72, 58.71 (4 × s, 1P). ³¹P{¹H} NMR (d_8 -toluene, 202 MHz, 223 K): δ 72.47, 70.27, 68.91, 58.75 (4 × s, 1P). 55 Mn{ 1 H} NMR (d_{8} -toluene, 124 MHz, 298 K): δ -718 (br. s). ⁵⁵Mn{¹H} NMR (d_8 -toluene, 124 MHz, 223 K): δ -812 (br. s). ⁵⁵Mn{¹H} NMR (d_8 -toluene, **124 MHz, 370 K)**: δ -601 (br. s). *trans*-5a: ν (N \equiv N): 1973 cm⁻¹, ν (Ge-H): 1860 cm⁻¹ (very broad). ¹H NMR (C₆D₆, 600 MHz, **298 K)**: δ 7.81 (d, 4H, ${}^{3}J_{H,H}$ 7.0 Hz, o-Ph), 7.12 (t, 4H, ${}^{3}J_{H,H}$ 7.3 Hz, m-Ph), 7.04 (t, 2H, ${}^{3}J_{H,H}$ 7.2 Hz, p-Ph), 4.74 (quin., 1H, ${}^{3}J_{H,P}$ 7.7 Hz, GeH), 1.80, 1.38 (2 × m, 4H, PCH₂), 1.29, 1.16 (2 × s, 12H, PC H_3). ¹³C{¹H} NMR (C₆D₆, 151 MHz, 298 K): δ 156.81 (s, i-Ph), 136.69 (s, o-Ph), 127.49 (s, m-Ph), 125.73 or 125.68 (s, p-Ph),§§ 31.35 (m, PCH₂), 20.28, 16.48 (2 × m, PCH₃). ³¹P{¹H} NMR (C₆D₆, 243 MHz, 298 K): δ 70.63 (br. s). ³¹P{¹H} NMR (d_8 toluene, 202 MHz, 223 K): δ 71.37 (s). ³¹P{¹H} NMR (d_8 toluene, 202 MHz, 370 K): δ 70.2 (broad multiplet with nearly indiscernible coupling due to quadrupolar collapse). ⁵⁵Mn{¹H} NMR (d_8 -toluene, 124 MHz, 298 K): δ -845 (br. s). ⁵⁵Mn{¹H} NMR (d_8 -toluene, 124 MHz, 223 K): δ –991 (br. s). ⁵⁵Mn{¹H} NMR (d_8 -toluene, 124 MHz, 370 K): δ -730 (br. s). Anal. found

(calcd): C, 47.25 (47.17); H, 7.14 (7.09); N, 4.42 (4.58).

Repetition of EA after 2.7 years sealed under argon at -30 °C:

Anal. found (calcd): C, 46.96 (47.17); H, 7.20 (7.09); N, 3.84 (4.58). $[(dmpe)_2Mn(GeHEt_2)(N_2)]$ (5b). 106.5 mg (0.22 mmol) of $[(dmpe)_2MnH(=GeEt_2)]$ (1b) was dissolved in 10 mL of benzene and transferred to a 100 mL storage flask. The mixture was freeze/pump/thawed three times, placed under 1 atm of N_2 at -95 °C, sealed, and warmed to room temperature. After stirring for 3 days at room temperature in the dark, the solvent was removed in vacuo. The resulting solid was recrystallized using 5 mL of hexanes at -30 °C to afford 65.3 mg (0.13 mmol, 58%) of cis-5b as yellow crystals. X-ray quality crystals of *trans*-5b were obtained by heating a mixture of approx. 10 mg of 1b under N₂ for 4 days at 60 °C in C₆D₆ (which resulted in cis-trans isomerization to a 22:78 ratio), followed by removal of the solvent in vacuo and recrystallization from a concentrated solution of hexanes at −30 °C. NMR spectra were obtained under an atmosphere of N_2 . *cis*-5b: $\nu(N \equiv N)$: 1989 cm⁻¹, ν (Ge-H): 1823 cm⁻¹. ¹H NMR (C₆D₆, 600 MHz, **298 K)**: δ 3.65 (m, 1H, GeH), 1.83, 1.82 (2 × t, 3H, ${}^{3}J_{H,H}$ 7.8 Hz, CH_2CH_3), 1.63 (m, 1H, PCH_2), 1.54 (d, 3H, ${}^2J_{H,P}$ 7.1 Hz, PCH_3), 1.23-1.56 (m, 4H, PC H_2), 1.50, 1.33, 1.32, 1.27 (4 × m, 1H, $C\underline{H}_2CH_3$) 1.47 (d, 3H, ${}^2J_{H,P}$ 6.7 Hz, $PC\underline{H}_3$), 1.14 (d, 3H, ${}^2J_{H,P}$ 6.3 Hz, PC H_3), 1.12 (d, 3H, ${}^2J_{H,P}$ 5.8 Hz, PC H_3), 1.06 (d, 3H, ${}^2J_{H,P}$ 6.5 Hz, $PC\underline{H}_3$), 1.03 (d, 3H, ${}^2J_{H,P}$ 5.9 Hz, $PC\underline{H}_3$), 0.97 (d, 3H, $^{2}J_{H,P}$ 5.0 Hz, PC H_{3}), 0.70-0.94 (m, 3H, PC H_{2}), 0.58 (d, 3H, $^{2}J_{H,P}$ 5.2 Hz, PC H_3). ¹³C{¹H} NMR (C₆D₆, 151 MHz, 298 K): δ 33.97 (m, PCH_2), 31.36 (app. t, $J_{C,P}$ 19.7 Hz, PCH_2), 28.90 (d of d, $J_{C,P}$ 23.5 and 16.4 Hz, PCH₂), 22.69 (app. d of t, $J_{C,P}$ 13.1 and 2.7 Hz, PCH₃), 21.99 (d of d, $J_{C,P}$ 13.1 and 5.0 Hz, PCH₃), 21.38 (d of m, $J_{C,P}$ 12.2 Hz, PCH₃), 20.98, 16.45 (2 × m, PCH₃), 20.64 (d, $J_{C,P}$ 13.9 Hz, PCH₃), 16.53, 16.02 (2 × s, CH₂CH₃), 15.78 (app. d of t, $J_{C,P}$ 20.7 and 3.3 Hz, PCH₃), 15.32 (d of d, $J_{C,P}$ 15.3 and 5.2 Hz, PCH₃), 12.47, 10.98 (2 × s, CH₂CH₃). ${}^{31}P{}^{1}H$ } NMR (C₆D₆, **243 MHz, 298 K)**: δ 75.51, 71.37, 65.43, 60.62 (4 × s, 1P). ³¹P $\{^{1}H\}$ NMR (d_{8} -toluene, 202 MHz, 223 K): δ 75.98, 71.85, 65.68, 60.76 (4 × s, 1P). ⁵⁵Mn{ 1 H} NMR (d_{8} -toluene, 124 MHz, 298 K): δ –1011 (br. s). ⁵⁵Mn{¹H} NMR (d_8 -toluene, 124 MHz, 223 K): δ -1070 (br. s). ⁵⁵Mn{¹H} NMR (d_8 -toluene, 124 MHz, 370 K): δ -906 (br. s). *trans*-5b: ν (N≡N): 1968 cm⁻¹ ν (Ge-H): not detected. ¹H NMR (C_6D_6 , 600 MHz, 298 K): δ 3.02 (m, 1H, GeH), 1.56, 1.34 (2 × m, 4H, PC H_2), 1.54 (t, 6H, ${}^3J_{H,H}$ 7.7 Hz, CH_2CH_3), 1.35, 1.21 (2 × s, 12H, PCH_3), 0.66 (m, 4H, CH_2CH_3). ¹³C(¹H) NMR (C₆D₆, 151 MHz, 298 K): δ 31.55 (quin, $J_{C,P}$ 11.7 Hz, PCH₂), 20.40, 16.53 (2 × m, PCH₃), 16.74 (s, CH₂CH₃), 15.38 (s, CH_2CH_3). ³¹P{¹H} NMR (C_6D_6 , 243 MHz, 298 K): δ 72.51 (m). ³¹P{¹H} NMR (d_8 -toluene, 202 MHz, 370 K): δ 71.79 (approx. 1:1:1:1:1:1 sextet, ${}^{1}J_{P,Mn}$ 274 Hz). ${}^{55}Mn\{{}^{1}H\}$ NMR (d_8 -toluene, 124 MHz, 298 K): δ –1094 (quin, ${}^1J_{P,Mn}$ 275 Hz). ⁵⁵Mn{¹H} NMR (d_8 -toluene, 124 MHz, 223 K): δ -1168 (s). ⁵⁵Mn{¹H} NMR (d_8 -toluene, 124 MHz, 370 K): δ –982 (quin, ¹J_{P,Mp} 274 Hz). **Anal.** found (calcd): C, 37.33 (37.31); H, 8.49 (8.42); N, 5.48 (5.44). Repetition of EA after 1000 days sealed in argon at -30 °C Anal. found (calcd): C, 37.16 (37.31); H, 8.56 (8.42); N, 5.10 (5.44).

Monitoring of conversion and cis: trans ratios for reactions of 1a-b with N_2 to form $[(dmpe)_2Mn(GeHR_2)(N_2)]$ (5a: R = Ph,

^{‡‡}This NMR signal could not be integrated because of overlap with a residual solvent signal.

^{§§} The p-Ph 13C NMR signals for the cis and trans isomers are too close in chemical shift to determine which signals correspond to which isomer.

Dalton Transactions

Den Access Article. Published on 11 Khotavuxika 2025. Downloaded on 2025-11-14 15:01:12.

This article is licensed under a Creative Commons Attribution-NonCommercial 3.0 Unported Licence.

5b: $\mathbf{R} = \mathbf{Et}$). Approx. 10 mg of $[(\text{dmpe})_2 \text{MnH}(=\text{GeR}_2)]$ (1a: $\mathbf{R} = \text{Ph}$, 1b: $\mathbf{R} = \text{Et}$) was dissolved in approx. 0.6 mL of C_6D_6 and the mixture was transferred to a J-young tube. The solutions were freeze/pump/thawed three times, placed under 1 atm of N_2 at -95 °C, sealed, and warmed to room temperature. Conversion of 1a-b to 5a-b, along with cis:trans ratios of 5a-b, were monitored by 1H NMR spectroscopy at various intervals. In the case of the reaction involving 1b, the reaction mixture was also heated at 60 °C for various times and monitored by 1H NMR spectroscopy.

 $[(dmpe)_2Mn(SiHPh_2)(N_2)]$ (6). Approx. 10 mg of a mixture containing [(dmpe)₂MnH(=SiPh₂)] and [(dmpe)₂MnH₂(SiHPh₂)] in a 6:1 ratio was dissolved in approx. 0.6 mL of C₆D₆ and the mixture was transferred to a J-young tube. The mixture was freeze/pump/thawed three times, placed under 1 atm of N2 at −95 °C, sealed, and warmed to room temperature. The resulting solution was analyzed by NMR spectroscopy in situ after sitting at room temperature for 2 hours, and contained $[(dmpe)_2MnH_2(SiHPh_2)]$, $cis-[(dmpe)_2Mn(SiHPh_2)(N_2)]$ (cis-6), and $trans-[(dmpe)_2Mn(SiHPh_2)(N_2)]$ (trans-6) in a 1:5.7:2.3 ratio. X-ray quality crystals of trans-6 were obtained by removing the solvent in vacuo, washing with 1 mL of hexanes, and recrystallization of the residue from 1 mL of toluene at −30 °C. *cis*-6 (selected): 1 H NMR (C₆D₆, 600 MHz, 298 K): δ 8.24 (d of d, 2H, ${}^{3}J_{H,H}$ 7.7 Hz, ${}^{4}J_{H,H}$ 1.3 Hz, o-Ph), 8.15 (d of d, 2H, ${}^{3}J_{H,H}$ 8.0 Hz, ${}^{4}J_{H,H}$ 1.3 Hz, o-Ph), 7.32 (t, 2H, ${}^{3}J_{H,H}$ 7.7 Hz, m-Ph), 7.24 (t, 2H, ${}^{3}J_{H,H}$ 7.6 Hz, m-Ph), 7.16 (m, 2H, p-Ph), 5.53 (m w. ${}^{29}Si$ sat., 1H, ${}^{1}J_{H,Si}$ 141 Hz, SiH), 1.35, 1.30 (2 × d, 3H, $J_{H,P}$ 6.6 Hz, PCH_3), 1.33 (d, 3H, $J_{H,P}$ 7.2 Hz, PCH_3), 1.17 (d, 3H, $J_{H,P}$ 5.6 Hz, PCH_3), 0.91 (d, 3H, $J_{H,P}$ 5.2 Hz, PCH_3), 0.90 (d, 3H, $J_{H,P}$ 4.7 Hz, PCH_3), 0.53 (d, 3H, $J_{H,P}$ 5.4 Hz, PCH_3). ¹³C{¹H} NMR (C₆D₆, **151 MHz, 298 K):** δ 152.75, 151.83 (2 × s, *i*-Ph), 137.25, 136.92 $(2 \times s, o-Ph)$, 127.18 (s, m-Ph), 126.14 (s, p-Ph), 34.25 (t, $J_{C,P}$ 21.8 Hz, PCH₂), 32.90, 32.06 (2 × m, PCH₂), 29.77 (d of d, $J_{C,P}$ 24.5 and 16.0 Hz, PCH₂), 24.71 (d of d, J_{C,P} 13.2 and 4.8 Hz, PCH_3), 23.05 (d of d, $J_{C,P}$ 13.2 and 6.3 Hz, PCH_3), 22.57 (m, $P\underline{C}H_3$), 19.75 (d, $J_{C,P}$ 19.7 Hz, $P\underline{C}H_3$), 16.86 (d, $J_{C,P}$ 18.4 Hz, PCH₃), 15.95 (d of d, $J_{C,P}$ 18.5 and 5.4 Hz, PCH₃), 15.26 (d of d, $J_{\rm C,P}$ 17.6 and 4.7 Hz, P<u>C</u>H₃). ²⁹Si NMR (data from ²⁹Si-¹H HMBC in C_6D_6 , 119 MHz, 298 K): δ 36.0. $^{31}P\{^1H\}$ NMR (C_6D_6 , **243 MHz, 298 K):** δ 71.78, 68.50, 64.12, 58.67 (4 × s, 1P). ⁵⁵Mn ${}^{1}H$ NMR (C₆D₆, 124 MHz, 298 K): δ -973 (br. s). ${}^{55}Mn{}^{1}H$ NMR (C₆D₆, 124 MHz, 360 K): δ –881 (br. s). *trans*-6: ¹H NMR (C₆D₆, 600 MHz, 298 K): δ 7.78 (d of d, 4H, ${}^{3}J_{H,H}$ 7.8 Hz, ${}^{4}J_{H,H}$ 1.4 Hz, o-Ph), 7.11 (t, 4H, ${}^{3}J_{H,H}$ 7.3 Hz, m-Ph), 7.04 (t of t, 2H, $^{3}J_{\rm H,H}$ 7.3 Hz, $^{4}J_{\rm H,H}$ 1.4 Hz, *p*-Ph), 4.82 (quin. w. $^{29}{
m Si}$ sat., 1H, $^{3}J_{H,P}$ 8.6 Hz, $^{1}J_{H,Si}$ 140 Hz, SiH), 1.79, 1.35 (2 × m, 4H, PCH₂), 1.27, 1.17 (2 × s, 12H, PC H_3). ¹³C{¹H} NMR (C₆D₆, 151 MHz, **298 K):** δ 154.10 (s, *i*-Ph), 136.39 (s, *o*-Ph), 127.31 (s, *m*-Ph), 126.01 (s, p-Ph), 31.31 (m, PCH₂), 20.55, 17.08 (2 × m, PCH₃). ²⁹Si NMR (data from ²⁹Si-¹H HMBC in C₆D₆, 119 MHz, 298 K): δ 33.9. ³¹P{¹H} NMR (C₆D₆, 243 MHz, 298 K): δ 70.8 (m). ³¹P ${}^{1}H$ NMR (C₆D₆, 202 MHz, 360 K): δ 70.39 (approx. 1:1:1:1:1:1 sextet, ${}^{1}J_{P,Mn}$ 269 Hz). ${}^{55}Mn\{{}^{1}H\}$ NMR (C₆D₆, **124 MHz, 298 K)**: δ -1098 (quin, ${}^{1}J_{P,Mn}$ 270 Hz). ${}^{55}Mn\{{}^{1}H\}$ **NMR** (C₆D₆, 124 MHz, 360 K): δ –1006 (quin, ${}^{1}J_{P,Mn}$ 270 Hz).

New spectroscopic for previously data $[(dmpe)_2MnH(=GeR_2)]$ (1a: R = Ph, 1b: R = Et) and $[(dmpe)_2MnH(=SiPh_2)].$ Approximately mg $[(dmpe)_2MnH(=GePh_2)]$ (1a), $[(dmpe)_2MnH(=GeEt_2)]$ (1b), or mixture of [(dmpe)₂MnH(=SiPh₂)] [(dmpe)₂MnH₂(SiHPh₂)] were dissolved in approx. 0.6 mL of (for 1a-b) d_8 -toluene or (for the silicon-containing species) C₆D₆, and analyzed by NMR spectroscopy. 1a: ⁵⁵Mn{¹H} NMR (d_8 -toluene, 124 MHz, 298 K): δ –1176 (br. s). ⁵⁵Mn{¹H} NMR (d_8 -toluene, 124 MHz, 370 K): δ –1107 (br. s). 1b: 55 Mn{ 1 H} NMR (d_8 -toluene, 124 MHz, 298 K): δ –1303 (br. s). ⁵⁵Mn{¹H} **NMR** (d_8 -toluene, 124 MHz, 370 K): δ -1226 (br. s). $[(dmpe)_2MnH(=SiPh_2)]:$ ⁵⁵Mn{¹H} NMR (C₆D₆, 124 MHz, **298 K)**: δ –548 (br. s).

Data availability

Data supporting this article is included in the ESI.† Crystallographic data for *trans*-2a/1a, *cis*-3a, *cis*-3b, *trans*-3c, 4, *cis*-5a, *trans*-5a, *cis*-5b, *trans*-5b, and 6 has been deposited at the CCDC with deposition numbers 2447494–2447503,† respectively.

Conflicts of interest

There are no conflicts to declare.

Acknowledgements

D. J. H. E. thanks NSERC of Canada for a Discovery Grant and Dr Yurij Mozharivskyj for access to his X-ray diffractometer. We are also grateful to Dr James Britten and Dr Gary Schrobilgen for helpful advice regarding X-ray crystal structures and analysis of NMR spectra involving coupling to quadrupolar nuclei, respectively, and Dr Novan Gray for assistance with high temperature NMR spectroscopy.

References

- 1 J. Baumgartner and C. Marschner, *Rev. Inorg. Chem.*, 2014, 34, 119–152.
- 2 V. Y. Lee, Eur. J. Inorg. Chem., 2022, e202200175.
- 3 M. Ghosh, N. Sen and S. Khan, *ACS Omega*, 2022, 7, 6449–6454.
- 4 T. J. Hadlington, Chem. Soc. Rev., 2024, 53, 9738-9831.
- 5 H. Hashimoto, T. Tsubota, T. Fukuda and H. Tobita, Chem. Lett., 2009, 38, 1196–1197.
- 6 H. Sakaba, Y. Arai, K. Suganuma and E. Kwon, *Organometallics*, 2013, 32, 5038–5046.
- 7 T. Fukuda, H. Hashimoto and H. Tobita, *J. Organomet. Chem.*, 2017, **848**, 89–94.
- 8 T. P. Dhungana, H. Hashimoto, M. Ray and H. Tobita, *Organometallics*, 2020, **39**, 4350–4361.

9 T. P. Dhungana, H. Hashimoto and H. Tobita, Dalton

- Trans., 2017, 46, 8167–8179.
- 10 M. Widemann, S. Jeggle, M. Auer, K. Eichele, H. Schubert, C. P. Sindlinger and L. Wesemann, *Chem. Sci.*, 2022, 13, 3999–4009.
- 11 K. K. Pandey, M. Lein and G. Frenking, *J. Am. Chem. Soc.*, 2003, 125, 1660–1668.
- 12 A. C. Filippou, U. Chakraborty and G. Schnakenburg, *Chem. Eur. J.*, 2013, **19**, 5676–5686.
- 13 A. C. Filippou, N. Weidemann, A. I. Philippopoulos and G. Schnakenburg, *Angew. Chem., Int. Ed.*, 2006, 45, 5987– 5991.
- 14 H. Hashimoto, T. Fukuda, H. Tobita, M. Ray and S. Sakaki, *Angew. Chem., Int. Ed.*, 2012, 51, 2930.
- 15 M. E. Fasulo and T. D. Tilley, Chem. Commun., 2012, 48, 7690–7692.
- 16 H. Hashimoto, T. Fukuda and H. Tobita, New J. Chem., 2010, 34, 1723–1730.
- 17 P. G. Hayes, R. Waterman, P. B. Glaser and T. D. Tilley, Organometallics, 2009, 28, 5082–5089.
- 18 S. Bajo, E. Soto, M. Fernández-Buenestado, J. López-Serrano and J. Campos, *Nat. Commun.*, 2024, **15**, 9656.
- 19 K. E. Litz, K. Henderson, R. W. Gourley and M. M. B. Holl, *Organometallics*, 1995, 14, 5008–5010.
- 20 S. Grumbine and T. D. Tilley, in *Progress in Organosilicon Chemistry*, ed. B. Marciniec and J. Chojnowski, Gordan and Breach, Amsterdam, 1995, pp. 133–146.
- 21 P. Gaspar and R. West, in *The Chemistry of Organic Silicon Compounds*, ed. Z. Rappoport and Y. Apeloig, John Wiley & Sons, Chichester, UK, 1998, vol. 2, ch. 43, pp. 2463–2568.
- 22 M. Okazaki, H. Tobita and H. Ogino, *Dalton Trans.*, 2003, 493–506.
- 23 R. Waterman, P. G. Hayes and T. D. Tilley, *Acc. Chem. Res.*, 2007, **40**, 712–719.
- 24 D. J. Cardin, B. Cetinkaya and M. F. Lappert, *Chem. Rev.*, 1972, 72, 545–574.
- 25 D. J. Cardin, B. Çetinkaya, M. J. Doyle and M. F. Lappert, *Chem. Soc. Rev.*, 1973, 2, 99–144.
- 26 T. Strassner, Top. Organomet. Chem., 2004, 1-20.
- 27 G. S. Girolami, G. Wilkinson, M. Thornton-Pett and M. B. Hursthouse, *J. Am. Chem. Soc.*, 1983, **105**, 6752–6753.
- 28 G. S. Girolami, C. G. Howard, G. Wilkinson, H. M. Dawes, M. Thornton-Pett, M. Motevalli and M. B. Hursthouse, J. Chem. Soc., Dalton Trans., 1985, 921–929.
- 29 J. S. Price, I. Vargas-Baca, D. J. H. Emslie and J. F. Britten, *Dalton Trans.*, 2023, **52**, 14880–14895.
- 30 J. S. Price, D. J. H. Emslie, I. Vargas-Baca and J. F. Britten, *Organometallics*, 2018, 37, 3010–3023.
- 31 J. S. Price, D. J. H. Emslie and J. F. Britten, *Angew. Chem., Int. Ed.*, 2017, **56**, 6223–6227.
- 32 J. S. Price and D. J. H. Emslie, *Chem. Sci.*, 2019, **10**, 10853–10869.
- 33 J. S. Price, D. J. H. Emslie and B. Berno, *Organometallics*, 2019, **38**, 2347–2362.
- 34 J. S. Price and D. J. H. Emslie, *Organometallics*, 2020, **39**, 4618–4628

- 35 H. M. Mobarok, R. McDonald, M. J. Ferguson and M. Cowie, *Inorg. Chem.*, 2012, 51, 4020–4034.
- 36 K. A. Smart, E. Mothes-Martin, L. Vendier, R. N. Perutz, M. Grellier and S. Sabo-Etienne, *Organometallics*, 2015, 34, 4158–4163.
- 37 P. M. Keil, S. Ezendu, A. Schulz, M. Kubisz, T. Szilvási and T. J. Hadlington, J. Am. Chem. Soc., 2024, 146, 23606–23615.
- 38 V. Y. Lee, R. Sakai, K. Takanashi, O. A. Gapurenko, R. M. Minyaev, H. Gornitzka and A. Sekiguchi, *Angew. Chem.*, *Int. Ed.*, 2021, 60, 3951–3955.
- 39 J. L. Vincent, S. Luo, B. L. Scott, R. Butcher, C. J. Unkefer, C. J. Burns, G. J. Kubas, A. Lledós, F. Maseras and J. Tomàs, *Organometallics*, 2003, 22, 5307–5323.
- 40 R. Herrmann, T. Braun and S. Mebs, *Eur. J. Inorg. Chem.*, 2014, 2014, 4826–4835.
- 41 A. Antiñolo, F. Carrillo-Hermosilla, A. Castel, M. Fajardo, J. Fernández-Baeza, M. Lanfranchi, A. Otero, M. A. Pellinghelli, G. Rima, J. Satgé and E. Villaseñor, Organometallics, 1998, 17, 1523–1529.
- 42 N. Zhang, R. S. Sherbo, G. S. Bindra, D. Zhu and P. H. M. Budzelaar, *Organometallics*, 2017, 36, 4123–4135.
- 43 J. Takaya and N. Iwasawa, Eur. J. Inorg. Chem., 2018, 2018, 5012–5018.
- 44 C. J. Laglera-Gándara, P. Ríos, F. J. Fernández-de-Córdova, M. Barturen, I. Fernández and S. Conejero, *Inorg. Chem.*, 2022, 61, 20848–20859.
- 45 M. A. Esteruelas, A. M. López, E. Oñate and E. Raga, *Angew. Chem., Int. Ed.*, 2022, **61**, e202204081.
- 46 U. Schubert, Adv. Organomet. Chem., 1990, 30, 151-187.
- 47 S. K. Ignatov, N. H. Rees, B. R. Tyrrell, S. R. Dubberley, A. G. Razuvaev, P. Mountford and G. I. Nikonov, *Chem. – Eur. J.*, 2004, **10**, 4991–4999.
- 48 P. Meixner, K. Batke, A. Fischer, D. Schmitz, G. Eickerling, M. Kalter, K. Ruhland, K. Eichele, J. E. Barquera-Lozada, N. P. M. Casati, F. Montisci, P. Macchi and W. Scherer, J. Phys. Chem. A, 2017, 121, 7219–7235.
- 49 S. Gründemann, H.-H. Limbach, G. Buntkowsky, S. Sabo-Etienne and B. Chaudret, *J. Phys. Chem. A*, 1999, **103**, 4752–4754.
- 50 R. H. Crabtree, Chem. Rev., 2016, 116, 8750-8769.
- 51 D. M. Heinekey, *J. Labelled Compd. Radiopharm.*, 2007, **50**, 1063–1071.
- 52 B. R. Bender, G. J. Kubas, L. H. Jones, B. I. Swanson, J. Eckert, K. B. Capps and C. D. Hoff, *J. Am. Chem. Soc.*, 1997, 119, 9179–9190.
- 53 G. Parkin, Acc. Chem. Res., 2009, 42, 315-325.
- 54 C. Perthuisot, M. Fan and W. D. Jones, *Organometallics*, 1992, **11**, 3622–3629.
- 55 C. R. Groom, I. J. Bruno, M. P. Lightfoot and S. C. Ward, *Acta Crystallogr., Sect. B*, 2016, 72, 171–179.
- 56 Y. Tanabe and Y. Nishibayashi, in *Transition Metal-Dinitrogen Complexes*, ed. Y. Nishibayashi, Wiley-VCH, Weinheim, Germany, 2019, ch. 1, pp. 1–77.
- 57 A. D. Piascik and A. E. Ashley, in *Transition Metal-Dinitrogen Complexes*, ed. Y. Nishibayashi, Wiley-VCH, Weinheim, Germany, 2019, ch. 6, pp. 285–335.

- 58 N. Mézailles, in *Transition Metal-Dinitrogen Complexes*, ed. Y. Nishibayashi, Wiley-VCH, Weinheim, Germany, 2019, ch. 4, pp. 221–269.
- 59 E. A. Ison, in *Transition Metal–Dinitrogen Complexes*, ed. Y. Nishibayashi, Wiley-VCH, Weinheim, Germany, 2019, ch. 5, pp. 271–284.
- 60 Q. Le Dé, D. A. Valyaev and A. Simonneau, *Chem. Eur. J.*, 2024, 30, e202400784.
- 61 D. Sellmann, Angew. Chem., Int. Ed. Engl., 1972, 11, 534– 534.
- 62 S. M. Howdle and M. Poliakoff, *J. Chem. Soc., Chem. Commun.*, 1989, 1099–1101.
- 63 J. A. Banister, P. D. Lee and M. Poliakoff, *Organometallics*, 1995, 14, 3876–3885.
- 64 P. D. Lee, J. L. King, S. Seebald and M. Poliakoff, *Organometallics*, 1998, 17, 524–533.
- 65 R. K. Merwin, A. C. Ontko, J. F. Houlis and D. M. Roddick, *Polyhedron*, 2004, **23**, 2873–2878.
- 66 J. A. Banister, M. W. George, S. Grubert, S. M. Howdle, M. Jobling, F. P. A. Johnson, S. L. Morrison, M. Poliakoff, U. Schubert and J. R. Westwell, *J. Organomet. Chem.*, 1994, 484, 129–135.
- 67 S. M. Howdle, M. A. Healy and M. Poliakoff, *J. Am. Chem. Soc.*, 1990, **112**, 4804–4813.
- 68 Y. Zheng, W. Wang, J. Lin, Y. She and K. Fu, *J. Phys. Chem.*, 1992, **96**, 9821–9827.
- 69 W. T. Boese and P. C. Ford, *Organometallics*, 1994, 13, 3525–3531.
- 70 J. B. Eastwood, L. A. Hammarback, M. T. McRobie, I. P. Clark, M. Towrie, I. J. S. Fairlamb and J. M. Lynam, *Dalton Trans.*, 2020, 49, 5463–5470.
- 71 B. H. G. Swennenhuis, R. Poland, N. J. DeYonker, C. E. Webster, D. J. Darensbourg and A. A. Bengali, Organometallics, 2011, 30, 3054–3063.
- 72 Y.-Q. Zou, S. Chakraborty, A. Nerush, D. Oren, Y. Diskin-Posner, Y. Ben-David and D. Milstein, *ACS Catal.*, 2018, 8, 8014–8019.
- 73 W. A. King, X.-L. Luo, B. L. Scott, G. J. Kubas and K. W. Zilm, *J. Am. Chem. Soc.*, 1996, **118**, 6782–6783.
- 74 W. A. King, B. L. Scott, J. Eckert and G. J. Kubas, *Inorg. Chem.*, 1999, 38, 1069–1084.
- 75 K. D. Welch, W. G. Dougherty, W. S. Kassel, D. L. DuBois and R. M. Bullock, *Organometallics*, 2010, 29, 4532– 4540.
- 76 P. DeShong, G. A. Slough, D. R. Sidler, P. J. Rybczynski, W. Von Philipsborn, R. W. Kunz, B. E. Bursten and T. W. Clayton Jr., *Organometallics*, 1989, 8, 1381–1388.
- 77 J. D. Cotton and R. D. Markwell, *Inorg. Chim. Acta*, 1990, 175, 187–191.
- 78 Z.-L. Xue and T. M. Cook, in *Comprehensive Inorganic Chemistry III*, ed. J. Reedijk and K. R. Poeppelmeier, Elsevier, Oxford, 3rd edn, 2023, pp. 660–744.
- 79 W. J. Miles Jr., B. B. Garrett and R. J. Clark, *Inorg. Chem.*, 1969, **8**, 2817.
- 80 B. Wrackmeyer, T. Hofmann and M. Herberhold, J. Organomet. Chem., 1995, 486, 255.

- 81 S. Onaka, T. Miyamoto and Y. Sasaki, *Bull. Chem. Soc. Jpn.*, 1971, 44, 1851.
- 82 W. Levason, S. D. Orchard and G. Reid, *Organometallics*, 1999, **18**, 1275–1280.
- 83 J. Connolly, M. K. Davies and G. Reid, *J. Chem. Soc.*, *Dalton Trans.*, 1998, 3833–3838.
- 84 J. Connolly, G. W. Goodban, G. Reid and A. M. Z. Slawin, J. Chem. Soc., Dalton Trans., 1998, 2225–2232.
- 85 W. Levason, L. P. Ollivere, G. Reid, N. Tsoureas and M. Webster, J. Organomet. Chem., 2009, 694, 2299–2308.
- 86 X.-X. Zhao, J. Wei and Z. Xi, *Chin. J. Chem.*, 2023, **41**, 2400–2407.
- 87 A. H. Klahn-Oliva, R. D. Singer and D. Sutton, *J. Am. Chem. Soc.*, 1986, **108**, 3107.
- 88 J. J. Carbó, O. Eisenstein, C. L. Higgitt, A. H. Klahn, F. Maseras, B. Oelckers and R. N. Perutz, J. Chem. Soc., Dalton Trans., 2001, 1452–1461.
- 89 J. A. Calladine, O. Torres, M. Anstey, G. E. Ball, R. G. Bergman, J. Curley, S. B. Duckett, M. W. George, A. I. Gilson, D. J. Lawes, R. N. Perutz, X.-Z. Sun and K. P. C. Vollhardt, *Chem. Sci.*, 2010, 1, 622–630.
- 90 D. Sellmann, Angew. Chem., Int. Ed. Engl., 1971, 10, 919-919.
- 91 Q. Le Dé, A. Bouammali, C. Bijani, L. Vendier, I. del Rosal, D. A. Valyaev, C. Dinoi and A. Simonneau, *Angew. Chem., Int. Ed.*, 2023, **62**, e202305235.
- 92 C. Barrientos-Penna and D. Sutton, *J. Chem. Soc., Chem. Commun.*, 1980, 111–112.
- 93 F. M. Bickelhaupt and E. J. Baerends, in *Rev. Comput. Chem*, ed. D. B. Boyd and K. B. Lipkowitz, Wiley-VCH, New York, 2000, pp. 1–86.
- 94 T. Ziegler and A. Rauk, Inorg. Chem., 1979, 18, 1755-1759.
- 95 T. Ziegler and A. Rauk, Inorg. Chem., 1979, 18, 1558-1565.
- 96 S. M. N. V. T. Gorantla and K. C. Mondal, *ACS Omega*, 2021, **6**, 33932–33942.
- 97 S. M. N. V. T. Gorantla and K. C. Mondal, *ACS Omega*, 2021, **6**, 33389–33397.
- 98 K. Devi, S. M. N. V. T. Gorantla and K. C. Mondal, *Eur. J. Inorg. Chem.*, 2022, **2022**, e202100931.
- 99 S. M. N. V. T. Gorantla, H. S. Karnamkkott, S. Arumugam, S. Mondal and K. C. Mondal, J. Comput. Chem., 2023, 44, 43–60.
- 100 H. S. Karnamkkott, S. M. N. V. T. Gorantla and K. C. Mondal, *J. Chem. Sci.*, 2024, **136**, 55.
- 101 P. W. Smith and T. D. Tilley, J. Am. Chem. Soc., 2018, 140, 3880–3883.
- 102 X. Yang and C. Wang, Angew. Chem., Int. Ed., 2018, 57, 923–928.
- 103 G. M. Bancroft, H. C. Clark, R. G. Kidd, A. T. Rake and H. G. Spinney, *Inorg. Chem.*, 1973, 12, 728.
- 104 F. Calderazzo, E. A. C. Lucken and D. F. Williams, *J. Chem. Soc. A*, 1967, 154.
- 105 M. K. Davies, M. C. Durrant, W. Levason, G. Reid and R. L. Richards, *J. Chem. Soc., Dalton Trans.*, 1999, 1077–1084.
- 106 J. Connolly, A. R. J. Genge, W. Levason, S. D. Orchard, S. J. A. Pope and G. Reid, *J. Chem. Soc., Dalton Trans.*, 1999, 2343–2352.

- 107 B. J. Burger and J. E. Bercaw, in Experimental Organometallic Chemistry - A Practicum in Synthesis and Characterization, American Chemical Society, Washington, D.C., 1987, vol. 357, pp. 79-98.
- 108 K. V. Zaitsev, I. P. Gloriozov, Y. F. Oprunenko, E. K. Lermontova and A. V. Churakov, I. Organomet. Chem., 2019, 897, 217-227.
- 109 R. K. Harris, E. D. Becker, S. M. Cabral de Menezes, R. Goodfellow and P. Granger, Pure Appl. Chem., 2001, 73, 1795-1818.
- 110 G. M. Sheldrick, Acta Crystallogr., Sect. A: Found. Adv., 2015, 71, 3-8.
- 111 G. M. Sheldrick, Acta Crystallogr., Sect. C: Struct. Chem., 2015, 71, 3-8.
- 112 O. V. Dolomanov, L. J. Bourhis, R. J. Gildea, J. A. K. Howard and H. Puschmann, J. Appl. Crystallogr., 2009, 42, 339-341.
- 113 ADF 2020.102, SCM, Theoretical Chemistry, Vrije Universiteit, Amsterdam, The Netherlands, https://www. scm.com.
- 114 G. te Velde, F. M. Bickelhaupt, E. J. Baerends, C. Fonseca Guerra, S. J. A. Van Gisbergen, J. G. Snijders and T. Ziegler, J. Comput. Chem., 2001, 22, 931-967.
- 115 J. P. Perdew, K. Burke and M. Ernzerhof, Phys. Rev. Lett., 1996, 77, 3865-3868.
- 116 E. van Lenthe, E. J. Baerends and J. G. Snijders, J. Chem. Phys., 1993, 99, 4597-4610.
- 117 E. van Lenthe, E. J. Baerends and J. G. Snijders, J. Chem. Phys., 1994, 101, 9783-9792.
- 118 E. van Lenthe, A. Ehlers and E.-J. Baerends, J. Chem. Phys., 1999, 110, 8943-8953.

- 119 E. van Lenthe, J. G. Snijders and E. J. Baerends, J. Chem. Phys., 1996, 105, 6505-6516.
- 120 E. van Lenthe, R. van Leeuwen, E. J. Baerends and J. G. Snijders, Int. J. Quantum Chem., 1996, 57, 281–293.
- 121 S. Grimme, J. Antony, S. Ehrlich and H. Krieg, J. Chem. Phys., 2010, 132, 154104.
- 122 S. Grimme, S. Ehrlich and L. Goerigk, J. Comput. Chem., 2011, 32, 1456-1465.
- 123 A. D. Becke, J. Chem. Phys., 1988, 88, 2547-2553.
- 124 M. Franchini, P. H. T. Philipsen and L. Visscher, J. Comput. Chem., 2013, 34, 1819-1827.
- 125 A. Bérces, R. M. Dickson, L. Y. Fan, H. Jacobsen, D. Swerhone and T. Ziegler, Comput. Phys. Commun., 1997, 100, 247-262.
- 126 H. Jacobsen, A. Bérces, D. P. Swerhone and T. Ziegler, Comput. Phys. Commun., 1997, 100, 263-276.
- 127 S. K. Wolff, Int. J. Quantum Chem., 2005, 104, 645-659.
- 128 T. Ziegler and A. Rauk, Inorg. Chem., 1979, 18, 1755-1759.
- 129 T. Ziegler and A. Rauk, Inorg. Chem., 1979, 18, 1558-1565.
- 130 M. Mitoraj and A. Michalak, Organometallics, 2007, 26, 6576-6580.
- 131 A. Michalak, M. Mitoraj and T. Ziegler, J. Phys. Chem. A, 2008, 112, 1933-1939.
- 132 M. P. Mitoraj, A. Michalak and T. Ziegler, Organometallics, 2009, 28, 3727-3733.
- 133 M. P. Mitoraj, A. Michalak and T. Ziegler, J. Chem. Theory Comput., 2009, 5, 962-975.
- 134 C. J. Jameson, in eMagRes, ed. R. K. Harris and R. L. Wasylishen, John Wiley & Sons, Ltd., 2007.
- 135 A. J. Jordan, C. M. Wyss, J. Bacsa and J. P. Sadighi, Organometallics, 2016, 35, 613-616.